



PB99-100117

REPORT FHWA/NY/RR-94/160



# Interpreting Data From the Falling-Weight Deflectometer

LUIS JULIAN BENDAÑA  
WEI-SHIH YANG  
DAN MCAULIFFE  
JIAN LU



RESEARCH REPORT 160

ENGINEERING RESEARCH AND DEVELOPMENT BUREAU  
NEW YORK STATE DEPARTMENT OF TRANSPORTATION  
Mario M. Cuomo, Governor/John C. Egan, Commissioner

REPRODUCED BY: **NTIS**  
U.S. Department of Commerce  
National Technical Information Service  
Springfield, Virginia 22161

## **STATE OF NEW YORK**

*Mario M. Cuomo, Governor*

## **DEPARTMENT OF TRANSPORTATION**

*John C. Egan, Commissioner*

*Michael J. Cuddy, Assistant Commissioner for Engineering and Chief Engineer*

*Paul J. Mack, Deputy Chief Engineer, Technical Services Division*

*Robert J. Perry, Director of Engineering Research and Development*

The Engineering Research and Development Bureau conducts and manages the engineering research program of the New York State Department of Transportation. The Federal Highway Administration provides financial and technical assistance for these research activities, including review and approval of publications.

Contents of research publications are reviewed by the Bureau's Director, and the appropriate section head. However, these publications primarily reflect the views of their authors, who are responsible for correct use of brand names and for the accuracy, analysis, and inferences drawn from the data.

It is the intent of the New York State Department of Transportation and the Federal Highway Administration that research publications not be used for promotional purposes. This publication does not endorse or approve any commercial product even though trade names may be cited, does not necessarily reflect official view or policies of either agency and does not constitute a standard, specification, or regulation.

## **ENGINEERING RESEARCH PUBLICATIONS**

*A. D. Emerich, Editor*

*Donna L. Noonan, Graphics and Production*

*Nancy A. Troxell and Jeanette M. LaClair, Copy Preparation*

INTERPRETING DATA FROM THE FALLING-WEIGHT DEFLECTOMETER

Luis Julian Bendaña, Engineering Research Specialist I  
Wei-Shih Yang, Engineering Research Specialist II  
Dan McAuliffe, Civil Engineer I  
Jian Lu, Engineering Research Specialist II

Final Report on Research Project 216-1  
Conducted in Cooperation With  
The U.S. Department of Transportation  
Federal Highway Administration  
Federal Technical Coordinator:  
Gary L. Owens

Research Report 160  
April 1994


PROTECTED UNDER INTERNATIONAL COPYRIGHT  
ALL RIGHTS RESERVED.  
NATIONAL TECHNICAL INFORMATION SERVICE  
U.S. DEPARTMENT OF COMMERCE

Reproduced from  
best available copy.



ENGINEERING RESEARCH AND DEVELOPMENT BUREAU  
New York State Department of Transportation  
State Campus, Albany, New York, 12232



1. Report No. FHWA/NY/RR-94/160		 PB99-100117		3. Recipient's Catalog No.	
4. Title and Subtitle INTERPRETING DATA FROM THE FALLING-WEIGHT DEFLECTOMETER				5. Report Date April 1994	
				6. Performing Organization Code	
7. Author(s) Luis Julian Bendana, Wei-Shih Yang, Dan McAuliffe, Jian Lu				8. Performing Organization Report No. Research Report 160	
9. Performing Organization Name and Address Engineering Research and Development Bureau New York State Department of Transportation State Campus, Albany, New York 12232				10. Work Unit No.	
				11. Contract or Grant No.	
12. Sponsoring Agency Name and Address Offices of Research, Development and Technology HRD-10 Federal Highway Administration U.S. Department of Transportation Washington, DC 20590				13. Type of Report and Period Covered Final Report Research Project 216-1	
				14. Sponsoring Agency Code	
15. Supplementary Notes Prepared in cooperation with the U.S. Department of Transportation, Federal Highway Administration. Study Title: Implementation of the Falling-Weight Deflectometer.					
16. Abstract  This publication compiles materials from a training program for interpreting data produced by the falling-weight deflectometer, a device that may gradually replace previous conventional methods for analyzing the structure and condition of existing pavements. The subjects covered include pavement response (basic theory including deflection, stain, and stress), empirical and mechanistic-empirical methods of pavement design, background and characteristics of the deflectometer and its measurements, backcalculation of material properties, and applications of the instrument in the context of revised AASHTO methods for overlay design.					
17. Key Words Deflectometer, deflection, testing, pavement response.			18. Distribution Statement No restrictions. This document is available to the public through the National Technical Information Service, Springfield, Virginia 22161.		
19. Security Classif. (of this report) Unclassified		20. Security Classif. (of this page) Unclassified		21. No. of Pages viii + 54	22. Price



## FOREWORD

The five modules presented here are a compiled version of a training program in use of the falling-weight deflectometer (FWD), conducted by the Engineering Research and Development Bureau. This program and report are intended to provide information necessary to understand analysis of pavement systems using the FWD, and analysis of the resulting data. The modules are summarized as follows:

- I. Pavement Response: this provides an overview of basics of elementary theory, Boussinesq's equations, layered systems, the Winkler foundation, and finite-element methods.
- II. Empirical and Mechanistic-Empirical Methods of Pavement Design: this discusses the basis for and differences between empirical and mechanistic-empirical design.
- III. The Falling-Weight Deflectometer: this gives background of deflection measurements and FWD characteristics.
- IV. Backcalculation of Material Properties: this reviews operational details of interpreting FWD data, and methods for backcalculation of layer moduli.
- V. Applications of the Falling-Weight Deflectometer: this discusses uses of the instrument and summarizes the revised AASHTO overlay design method.





## CONTENTS

I.	PAVEMENT RESPONSE . . . . .	1
	A. Basics of the Theory of Elasticity . . . . .	1
	B. Bossinesq's Equations . . . . .	2
	C. Layered Systems . . . . .	4
	D. The Winkler Foundation . . . . .	5
	E. Basics of the Finite-Element Method (FEM) . . . . .	7
II.	EMPIRICAL AND MECHANISTIC-EMPIRICAL METHODS OF PAVEMENT DESIGN . .	11
	A. The Empirical Approach . . . . .	11
	B. The Mechanistic-Empirical Approach . . . . .	12
	C. Comparison of the Two Approaches . . . . .	12
III.	THE FALLING-WEIGHT DEFLECTOMETER . . . . .	19
	A. Background of Deflection Measurements . . . . .	19
	B. The Benkelman Beam (Static Deflection) . . . . .	19
	C. The Dynaflect (Steady-State Vibration) . . . . .	20
	D. The Falling-Weight Deflectometer (Dynamic Deflection) . . . . .	20
	E. FWD Calibration (The SHRP Procedure) . . . . .	24
	F. Further Research . . . . .	24
IV.	BACKCALCULATION OF MATERIAL PROPERTIES . . . . .	27
	A. Deflection Data Analysis . . . . .	27
	B. Programs for Backcalculation . . . . .	34
V.	APPLICATIONS OF THE FALLING-WEIGHT DEFLECTOMETER . . . . .	37
	A. Benefits for Pavement Management Systems . . . . .	38
	B. Design Procedures . . . . .	38
	C. Other Uses . . . . .	49
	REFERENCES . . . . .	51

Figure 1. Stress-strain curve for an elastic material.

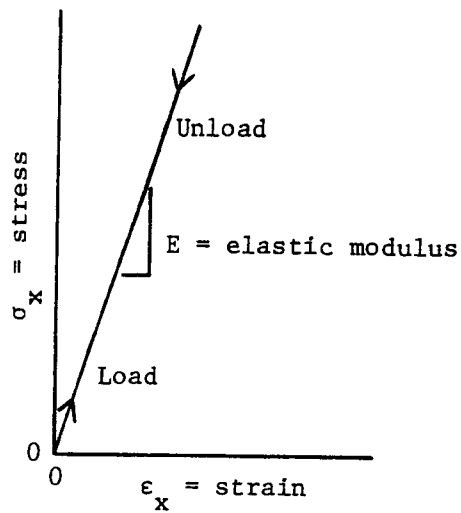
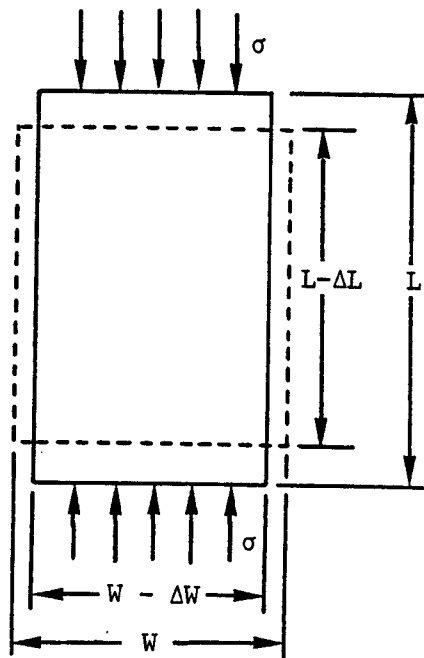


Figure 2. Definition of coefficient of elasticity and Poisson's ratio for uniaxial case.



## MODULE I: PAVEMENT RESPONSE

### A. Basics of the Theory of Elasticity

Pavement structural responses (deflections, strains, stresses) due to FWD loading have been compared to those of a truck wheel moving at about 60 km/h. Test results indicate that these responses are almost identical. The theory of elasticity is one method of estimating these responses to applied loads. It assumes that if a body is perfectly elastic, deformation occurs when an external force is applied, but disappears with removal of that force. In the theory's simplest version, two material properties are used: E (modulus of elasticity) and  $\nu$  (Poisson's ratio). Hook's law states that the ratio of stress over strain is a constant (Fig. 1), and that E is found as follows:

$$E = \frac{\sigma_x}{\epsilon_x} \quad (1)$$

where  $\sigma_x$  = stress in the x direction, and

$\epsilon_x$  = strain in the x direction.

Poisson's ratio is the ratio of radial to longitudinal strain (Fig. 2) and is found as follows:

$$\nu = \frac{\epsilon_r}{\epsilon_L} \quad (2)$$

$$\epsilon_r = \frac{\Delta W}{W} \quad (3)$$

$$\epsilon_L = \frac{\Delta L}{L} \quad (4)$$

where  $\epsilon_r$  = radial strain,

$\epsilon_L$  = longitudinal strain,

W = initial width,

$\Delta W$  = change in width,

$L$  = initial length, and

$\Delta L$  = change in length.

### B. Boussinesq's Equation

Closed-form solutions to compute pavement stress are based on the theory of elasticity. For general three-dimensional structures, use of the basic equations introduces fifteen unknown variables: six strains, six stresses, and three displacements. To find an exact solution, these unknowns must satisfy six strain-displacement equations, six stress-strain equations, and three equations of equilibrium. Exact solutions for most problems thus are usually complex, and knowledge of differential equations is necessary to obtain them for even the most elementary problems. However, to analyze pavements, many formulas have been derived from this theory. These formulas are all similar and differ only in assumptions made to represent material properties and geometry. The discussion here is restricted to one of the most widely used formulas, published in 1885 by Boussinesq, a French mathematician (1). His equation related vertical stress at any depth below the earth's surface to a point load at the surface:

$$\sigma_z = k \frac{P}{z^2} \quad (5)$$

$$\text{where } k = \frac{3}{2} \pi [1 + (r/z)^2]^{-5/2},$$

$\sigma_z$  = vertical stress, MPa,

$r$  = radial distance from the point load, mm,

$z$  = depth, mm, and

$p$  = point load, N.

Stresses can also be computed in polar coordinates:

$$\sigma_r = \frac{3P \cos \theta}{2\pi R^2} \quad (6)$$

$$\sigma_r = \left[ \frac{P(3 \cos \theta \sin^2 \theta) - (1 - 2\nu)}{(1 + \cos \theta)} \right] \frac{1}{2\pi R^2} \quad (7)$$

$$\sigma_t = \left[ \frac{P(1 - 2\nu) \frac{(1 - \cos \theta)}{(1 + \cos \theta)}}{2\pi R^2} \right] \quad (8)$$

$$\tau_{rz} = \frac{3P(\cos^2 \theta \sin \theta)}{2\pi R^2} \quad (9)$$

$$\epsilon_z = \frac{[(1 + \nu)P(3 \cos^3 \theta - 2\nu \cos \theta)]}{2\pi R^2 E} \quad (10)$$

$$d_z = \frac{[(1 + \nu)P(2(1 - \nu) + \cos^2 \theta)]}{2\pi R E} \quad (11)$$

where P = point load,

$\theta$  = angle from z axis to point load,

R = radial distance from point load,

$\sigma_r$  = radial stress, MPa,

$\sigma_t$  = tangential stress, MPa,

$\tau$  = shear stress, MPa,

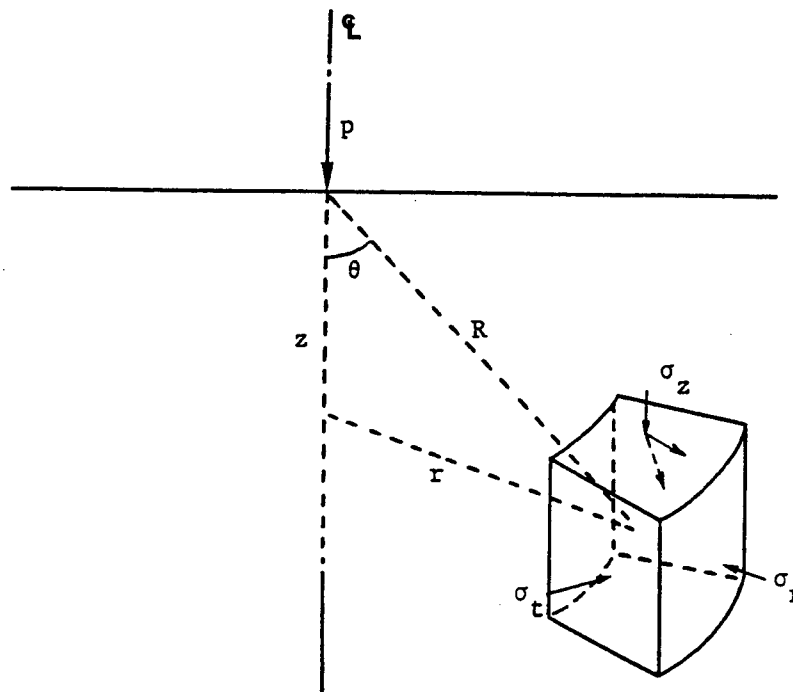
$\epsilon$  = strain,

$d_z$  = displacement in the z direction,

$\nu$  = Poisson's ratio, and

E = elastic modulus.

Figure 3. Stress components.



Physical interpretation of the components of stress is shown in Figure 3. Here are three observations from the Boussinesq equations:

1. Vertical stress is independent of material properties and depends only on depth, radial distance, and point load.
2. Maximum stress occurs directly under the load.
3. Stresses decrease with depth and radial distance.

Difficulty is encountered when the equations are used to compute stresses due to tire pressure, since they consider only concentrated loads. To overcome this problem, early in the 20th century the solution for a point load on a semi-infinite half-space was generalized to loads distributed over areas of general shapes.

### C. Layered Systems

Burmister (2) extended Boussinesq's solution to two-layer elastic systems. His solutions assumed that materials in the layers are homogeneous, isotropic,

incompressible, and elastic. Acum and Fox (3) extended Burmister's solution to the three-layer case. The first two programs capable of analyzing up to five layers, loaded by a point load or a circular load, were presented in 1959 by Mehta and Veletsos (4). Since then, other programs have been developed for multi-layer elastic analysis, including the following:

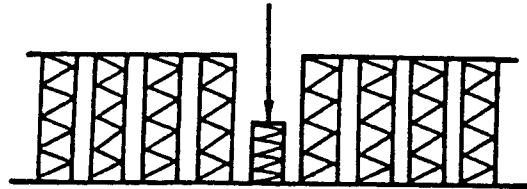
1. CHEVRON, a program written in the early 1960s, used the theoretical background outlined by Michelow (5) and constituted an enhancement of the work of Mehta and Veletsos. This program computes vertical, tangential, radial, and shear stresses, and vertical and radial strains, and was limited to five layers. In 1967, it was expanded to handle a maximum of fifteen layers, and in 1980 modifications were introduced to improve its accuracy. The CHEVRON model was used in developing the mechanistic-empirical Thickness Design Manual of the Asphalt Institute (6).
2. ELSYM5 is an expanded version of the CHEVRON program. The new capabilities include computation of displacements and principal stresses, and ability to handle multi-wheel loads.
3. BISTRO is the precursor of another family of programs for layered elastic analysis. Theoretical derivation for BISTRO follows work by Schiffman (7). It can calculate stresses, strains, and displacements, assuming rough interfaces between layers, and can account for multi-wheel loads.
4. BISAR is a new version of BISTRO, expanded in the 1970s to accommodate tangential surface loadings and include layer interfaces. It is a structural model program developed by Shell International Petroleum Company Limited, and used in their Pavement Design Manual (8).

#### D. The Winkler Foundation

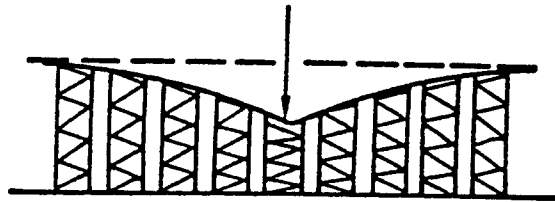
Layered elastic theory does not account for discontinuities in layers, and thus cannot be applied for analysis of rigid pavement at or near slab joints, where critical stresses occur. Westergaard overcame this problem by introducing the theory of the Winkler Foundation in analyzing pavement slabs on grade. This theory, also known as the dense liquid model, assumes that the subgrade cannot transfer shear stresses (Fig. 4) -- that is, the soil is considered to be composed of independent linear springs. It is also assumed that vertical stress

Figure 4. A Winkler (or dense-liquid) foundation and an elastic solid subgrade foundation.

A. Winkler Foundation (no shear transfer)



B. Elastic Solid Subgrade Foundation (with shear transfer)



at any point on the foundation is directly proportional to vertical deflection at that point (Eq. 12). This theory is attributed to Winkler (9) and is known as "the Winkler Foundation":

$$\sigma = kv \quad (12)$$

where  $\sigma$  = vertical stress, kPa,

$k$  = modulus of subgrade reaction, MPa/m, and

$v$  = vertical deflection, mm.

Westergaard developed a set of equations for analysis of rigid pavement on dense liquid for corner loads, edges loads, and interior loads. Influence charts were also developed and presented by Yoder (10). With state-of-the-art computer systems, a more realistic representation of slab-on-grade has been accomplished using three-dimensional finite-element programs. "Illi-slab" (11) developed at the University of Illinois is such a program, capable of a variety of support



characterization models, including dense-liquid and stress-dependent subgrade models.

#### E. Basics of the Finite-Element Method (FEM)

In this method, as in the classic elasticity approach, one must use the basic equations of elasticity, but the actual continuous structure is assumed to be represented by a model composed of an assemblage of a finite number of simple elements. These are analyzed separately as determinate members, and appropriate force-displacement relations are written. These individual elements are then interconnected at nodal points where force and displacement compatibility is required, and the assemblage of these elements forms the pavement structure.

FEM treats displacements at the joints of individual elements as unknowns, and the problem is formulated by considering component matrices for each element, which when combined according to compatibility rules yield a set of matrix equations that describe behavior of the idealized structural system.

In calculating displacements by FEM, a large system of algebraic equations must be solved (Eq. 13), one for each degree of freedom:

$$[K]\{v\} = \{F\} \quad (13)$$

where  $[K]$  =  $n \times n$  stiffness matrix,

$\{v\}$  =  $n \times 1$  unknown displacements, and

$\{F\}$  =  $n \times 1$  nodal forces.

When a structure and its external loads are axisymmetric, the stress components are independent of the angular ( $\theta$ ) coordinate; thus all derivatives with respect to ( $\theta$ ) vanish.

To write equilibrium equations for a single element that has been cut from the indeterminate structure, one must evaluate the stiffness matrix. To calculate its coefficients, the expression for the internal potential  $U$  (strain energy due to deformation of the element) must be obtained.

Stiffness coefficients are defined as the second partial derivative of  $U$  with respect to displacement:

$$K_{ij} = \frac{\delta^2 U}{\delta v^2} \quad (14)$$

Strain energy  $U$  is given as follows:

$$U = \frac{1}{2} \int_{\text{vol}} [\sigma] \{\epsilon\} dV \quad (15)$$

where  $[\sigma]$  - a row of vectors of stresses,

$\{\epsilon\}$  - a column of vectors of strains, and

$$dV = r dr d\theta dz.$$

The constitutive relation is given as follows:

$$\{\sigma\} = [D] \{\epsilon\} \quad (16)$$

where  $\{\sigma\}$  - a column of vectors of stresses,

$[D]$  - the elasticity matrix (linking  $\sigma$  and  $\epsilon$ ), and

$\{\epsilon\}$  - a column of vectors of strains.

Strain displacement equations in cylindrical coordinates are given by the following six equations:

$$\epsilon_r = \frac{\delta \mu}{\delta r} \quad (17)$$

$$\epsilon_\theta = \frac{\mu}{r} + \left(\frac{1}{r}\right) \frac{\delta v}{\delta \theta} \quad (18)$$

$$\epsilon_z = \frac{\delta w}{\delta z} \quad (19)$$

$$\gamma_{zr} = \frac{\delta \mu}{\delta z} + \frac{\delta w}{\delta r} \quad (20)$$

$$\gamma_{r\theta} = \left(\frac{1}{r}\right) \frac{\delta \mu}{\delta \theta} + \frac{\delta \gamma}{\delta r} - \frac{v}{r} \quad (21)$$

$$\gamma_{\theta z} = \left( \frac{1}{r} \right) \frac{\delta w}{\delta \theta} + \frac{\delta v}{\delta z} \quad (22)$$

where  $\mu$  = displacement in the r direction,

$r$  = distance from point load application to point of interest,

$v$  = displacement in the  $\theta$  direction,

$w$  = displacement in the z direction,

$\delta z$  = initial incremental length of z,

$\delta w$  = initial incremental length of w,

$\delta \theta$  = initial incremental length of  $\theta$ ,

$\theta$  = angle to point of interest,

$\gamma_{zr}$  = displacement in the zr direction,

$\gamma_{r\theta}$  = displacement in the r $\theta$  direction, and

$\gamma_{\theta z}$  = displacement in the  $\theta z$  direction,

$\epsilon_r$  = strain in the r direction,

$\epsilon_z$  = strain in the z direction, and

$\epsilon_\theta$  = strain in the  $\theta$  direction.

Substituting Eqs. 17 through 22 into Eq. 15 and integrating, the strain energy U is obtained as a function of the displacements. Taking the first and second derivatives with respect to v (displacements) of the strain energy U, one obtains the stiffness coefficients and then the equation of equilibrium (Eq. 13) is used to solve for unknown displacements.



## MODULE II: EMPIRICAL AND MECHANISTIC-EMPIRICAL METHODS OF PAVEMENT DESIGN

### A. The Empirical Approach

Empirical observations have always provided the basis for formulating criteria to be applied in practice. The first important full-scale accelerated pavement experiment was conducted at Ottawa, Illinois in the 1950s, and was known as the AASHO Road Test (12). The AASHTO design procedure (13) is based on data collected then, and takes into account a number of design and behavioral factors under test loads.

This approach is based on ability of the pavement to serve traffic over a period of time and is known as its functional performance, which is measured by an index called the Present Serviceability Index (PSI). This is a numerical value ranging from 5 (representing the best possible pavement) down to 0 (representing no pavement at all). In the AASHO Road Test it was assumed that pavement deflection under load was directly related to loss of PSI.

For example, the AASHO 80-kN ESAL (equivalent single-axle load) factors were derived for dual-tire single and tandem axles, with a maximum single-axle load of 133 kN and tandem-axle load of 214 kN. AASHO equivalency factors thus are limited to these axle configurations and load ranges. The 1986 AASHTO Guide (13) for design of pavement structures is used by many states, but due to limitations of the data from the AASHO Road Test, many factors provided are outside the boundaries from which they were developed. Obviously, problems arise when functional methods are used if there are no experimental data to support their use. A solution to this problem is using a combination of empirical and mechanistic methods -- this is, using a mechanistic model, calibrated empirically by field data, to evaluate damaging effects of traffic and environment.

### B. The Mechanistic-Empirical Approach

Part IV of the 1986 AASHTO Guide (13) states:

Mechanistic design procedures are based on the assumption that a pavement can be modeled as a multi-layered elastic or visco-elastic structure on an elastic or visco-elastic foundation. Assuming that pavements can be modeled in this manner, it is possible to calculate the stress, strain, or deflection (due to traffic loadings and/or environments) at any point within or below the pavement structure. However, researchers recognize that pavement performance will likely be influenced by a number of factors which will not be precisely modeled by mechanistic methods. It is, therefore, necessary to calibrate the models with observations of performance, i.e., empirical correlations. Thus, the procedure is referred to in the Guide as a mechanistic-empirical design procedure.

For flexible pavements, this approach assumes that structural failures are caused by fatigue cracking associated with horizontal tensile strain (Fig.5) and rutting, which can be related to vertical compressive strain -- that is, mechanistic procedures have been applied to cracking and rutting predictions. The assumption is that maximum compressive or tensile strains and performance are unique, regardless of the type of axle configuration. For fatigue cracking, the approach empirically relates fatigue life (total ESALs) to maximum tensile stress ( $\sigma_{max}$ ) or tensile strain ( $\epsilon_{max}$ ) occurring on the underside of the pavement when loaded by traffic. For permanent deformation, this approach relates fatigue life to plastic or permanent strain in each pavement layer. Total deformation is estimated by summing deformations over the full depth.

For rigid pavement, the mechanistic-empirical procedure has been applied to determine joint spacing, dowel size, and size and placement of reinforcing steel.

### C. Comparison of the Two Approaches

#### 1. Problem

Design an experiment to find how rigid pavement faulting depends on its geometry, material properties, temperature, and the load acting on it.

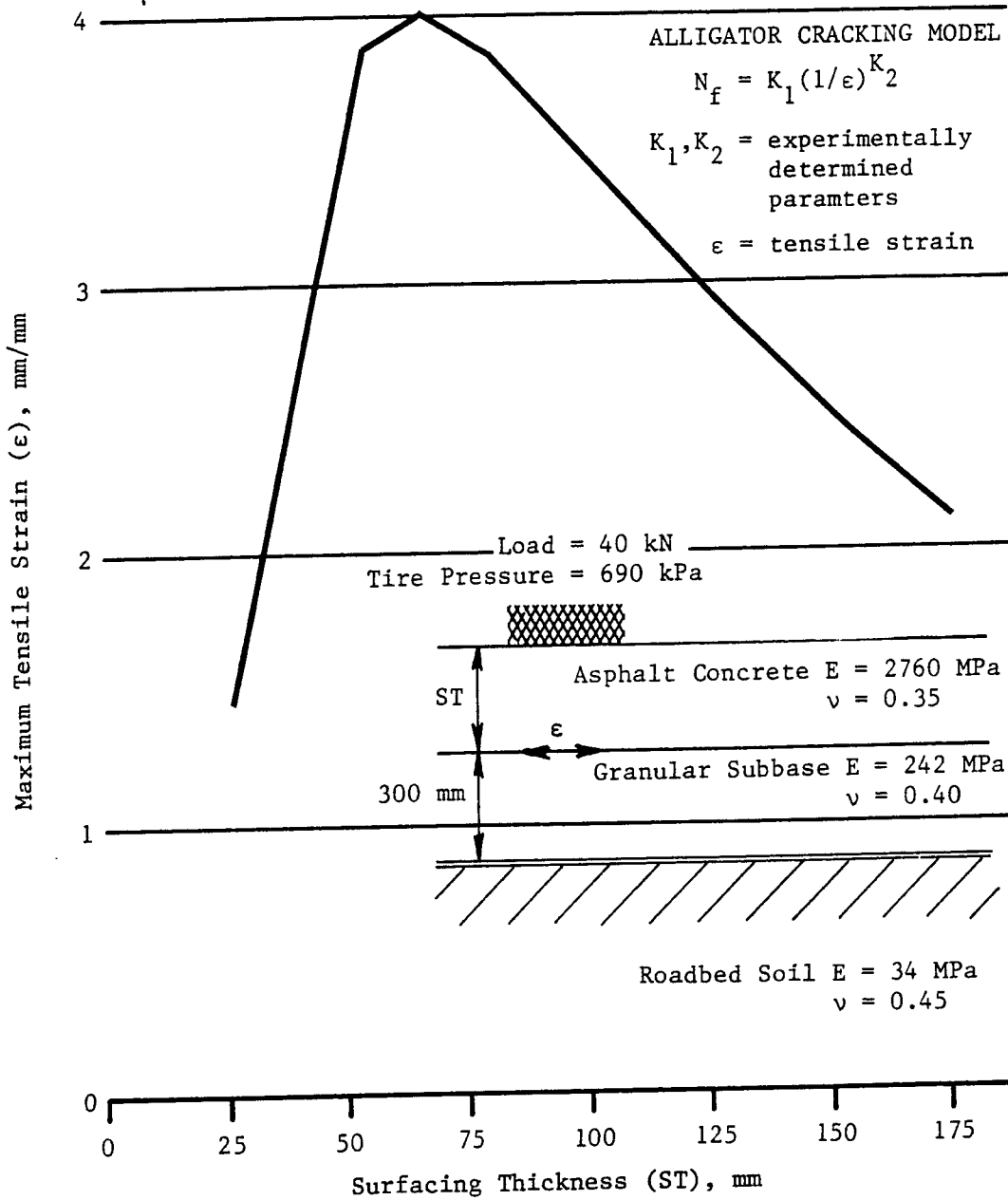
Fatigue:  $N$  = number of 80-kN ESALs

Load:  $P$  = shear force acting on the dowel ( $F$ )

Material Properties:

$E_d$  = modulus of elasticity of the dowel ( $FL^{-2}$ )

Figure 5. Maximum tensile strain vs. surfacing thickness.



Surfacing Thickness (ST), mm	$\epsilon \times 10^{-4}$ mm/mm
25	1.43
50	3.87
63	4.00
75	3.88
100	3.41
125	2.91
150	2.47
175	2.10

$K_s$  = soil modulus of subgrade reaction (FL<sup>-3</sup>)

$K_c$  = modulus of dowel support (FL<sup>-3</sup>)

C = slab subbase frictional restraint

Geometry:

L = slab length (L)

TS = shoulder type

d = dowel diameter (L)

Temperature:

$\Delta T$  = mean temperature range (°C)

2. Solution by the Empirical Approach

1 dependent variable: faulting

10 independent variables: ESALs, P,  $E_d$ ,  $K_s$ ,  $K_c$ , C, L, TS, d,  $\Delta T$

2 or 3 levels of each variable

2<sup>10</sup> or 3<sup>10</sup> total tests

1024 or 59049: full factorial

Equation:

1. Linear Regression Model

$$\text{Fault} = a + b(\text{ESALs}) + c(P) + d(E_d) + e(K_s), f(K_c) + \dots + g(C) + h(L) + i(\text{TS}) + j(d) + k(\Delta T) \quad (23)$$

2. Non-linear Regression Model

$$\text{Fault} = \text{ESALs}^a [ b (P^c E_d^d K_c^e C^f L^g d^h \Delta T^i) K_s^j \text{TS}^k ] \quad (24)$$



### 3. Mechanistic-Empirical Approach

In 1938, a procedure was presented by Friberg (14) to calculate maximum concrete bearing stress ( $\sigma_{\max}$ ):

$$\sigma_{\max} = \frac{K_c P (2 + \beta\omega)}{4\beta^3 E_d I} \quad (25)$$

$$\text{where } \beta = \left[ \frac{K_c d}{4 E_d I} \right]^{\frac{1}{4}},$$

$\beta$  = relative stiffness of concrete around the dowel ( $L^{-1}$ ),

$K_c$  = modulus of dowel support ( $FL^{-3}$ ),

$d$  = dowel diameter (L),

$E_d$  = modulus of elasticity of the dowel ( $FL^{-2}$ ),

$P$  = shear force acting on the dowel (F),

$I$  = moment of inertia of the dowel ( $L^3$ ),

$\omega = CL [0.5\alpha_t \Delta T + \epsilon_s]$ ,

where  $\omega$  = joint opening (L).

$C$  = slab subbase frictional restraint,

$L$  = slab length (L),

$\alpha_t$  = coefficient of thermal expansion of the concrete slab ( $^{\circ}C^{-1}$ ),

$\Delta T$  = mean temperature range ( $^{\circ}C$ ), and

$\epsilon_s$  = coefficient of drying shrinkage of the concrete slab.

In the late 1970s, with the aid of the finite-element method Tabatabaie et al. (15) found that dowel diameter and elastic modulus of the concrete have significant effects on maximum concrete bearing stress. They derived the following relationship for maximum concrete bearing stress:

$$\sigma_{\max} = \frac{(5515.808 + 0.068E_c)}{d^{\frac{4}{3}}} (25.4 + 0.35\omega) LT \quad (26)$$

where  $E_c$  = modulus of elasticity of the concrete, MPa,

$d$  = dowel diameter, mm,

$\omega$  = joint opening, mm,

LT =  $SP\alpha$ , maximum load transferred by a dowel, kN,

$S$  = dowel spacing, mm,

$P$  = applied external load, kN, and

$\alpha$  = 0.0091 for edge load,

= 0.0116 for protected corner load,

= 0.0163 for unprotected corner load.

Also, using a finite-element program, maximum concrete bearing stress can be calculated. Independent of the procedure if the law of mechanics is used the number of independent variables is reduced to four:

Dependent Variable: 1 (Fault)

Independent Variables: 4 (ESALs,  $K_s$ , TS, and  $\sigma_{\max}$ )

Levels of Each Variable: 2 or 3

Number of Tests:  $2^4$  or  $3^4$

Full Factorial: 16 or 81

The Eq. 27 model was formulated using data from the AASHO Road Test, a database developed by ERES for FHWA (16), and COPEs (17). These data include various pavement characteristics, environmental conditions, and traffic conditions:

$$\text{Fault} = \text{ESALs}^a (b\sigma_{\max}^c + dk^e + fTS) \quad (27)$$

where Fault = mean transverse joint faulting, mm,

ESALs = number of cumulative 80-kN ESALs, millions,

$\sigma_{\max}$  = maximum concrete bearing stress, MPa,

k = modulus of subgrade reaction, MPa/m, and

TS = shoulder type (0 if a bituminous shoulder, 1 if a tied shoulder).

Estimated coefficients are:

a = 0.6

b = 0.01784604

c = 2

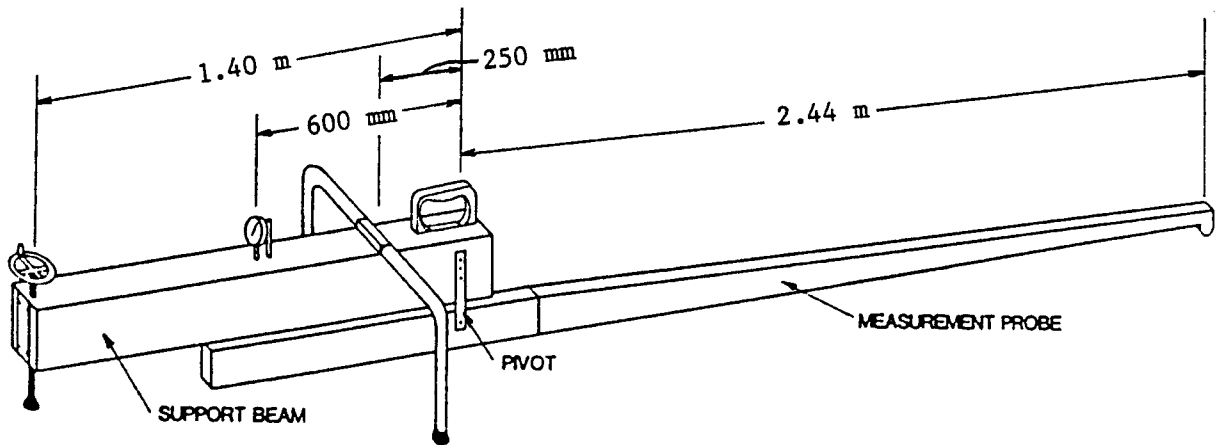
d = 144.6

e = -1.809

f = -0.0074

This example has demonstrated that using engineering principles -- that is, a procedure based on the laws of mechanics, resulting in a designed experiment with full factorial for Level 2 of each variable -- the number of tests is reduced from 1024 to 16.

Figure 6. The Benkelman beam.



## MODULE III: THE FALLING-WEIGHT DEFLECTOMETER

### A. Background of Deflection Measurement

Pavement management systems (PMSs) have been developed throughout the United States over the last 20 years and have been adopted in many states. Current technologies allow measurement of five PMS variables:

1. Roughness,
2. Rutting,
3. Skid resistance,
4. Pavement deflection, and
5. Pavement distress.

In the field, data for these variables can be collected automatically by computerized instrumentation systems. In the last 40 years, many devices have been developed to measure deflection, including the Benkelman beam, the Dynaflect, and the falling-weight deflectometer. The primary purpose of deflection measurement is to collect information concerning the pavement structure. The major variables to be estimated are elastic modulus (E values), foundation support (k values or CBR), and degree of load transfer (J factors). This information can be used for design of new and reconstructed pavements, joints, and overlays.

### B. The Benkelman Beam (Static Deflection)

This device (Fig. 6) measures pavement response to a static load. When a given load (usually a truck loaded with selected weights) is applied to the pavement where deflection is to be measured, the beam reading is adjusted to zero. The

load is then removed, resulting in a beam reading indicating the deflection caused by the known static load. The traditional Benkelman beam must be manually balanced and read.

### C. The Dynaflect (Steady-State Vibration)

Shown in Figure 7, this machine produces sine-function vibration transmitted to the pavement through steel wheels. Pavement response to the force of vibration is measured at various positions by sensors called geophones. The physical variables measured by the sensors are vertical velocities of the pavement surface at various positions (Fig. 8). Because the force input to the pavement structure is sinusoidal, pavement response is considered to be steady-state, allowing control of the data collection procedure by a microcomputer system that can also process the collected data. The Dynaflect has two sets of wheels -- an outer set for transport, and an inner (steel) set for testing. When the system is not in operation the steel wheels are lifted, and during testing the outer wheels are lifted and the steel wheels fully contact the pavement so that vibration force can be effectively transmitted.

### D. The Falling-Weight Deflectometer (Dynamic Deflection)

In the United States some of the more popular FWD models are known commercially as the Dynatest, KUAB, and Phoenix. They lift weights to predetermined heights and then drop them on a loading plate, producing an impulse force that in turn can be controlled by adjusting the height from which the weights are released. Sensors on the deflectometer measure vertical velocities of the pavement surface, thus recording pavement response to the impact load. When the falling weights touch the loading plate, an impulse force is produced (Fig. 9) and measured by the sensors. The intermediate characteristics, including magnitude of response, transit time, and duration, are dependent on pavement materials and impact load. If other conditions are fixed, the waveforms measured by the sensors may be used to estimate materials characteristics.

Sensors may be distributed uniformly or non-uniformly (Fig. 10). Because the form of the deflection basin changes most around the point where the impulse force is applied, more sensors are needed in that region and non-uniform distribution thus is used more often. Figure 11 shows the process of measuring the deflection basin. When an impulse force is applied, pavement response is measured at various locations by geophones. Using an integrator, vertical

Figure 7. Dynaflect with rubber outer wheels and steel (rigid) inner wheels.

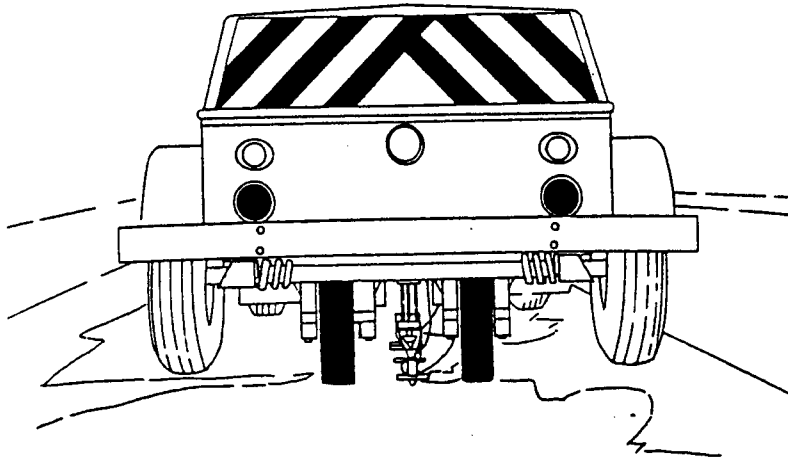


Figure 8. Distribution of Dynaflect geophone sensors.

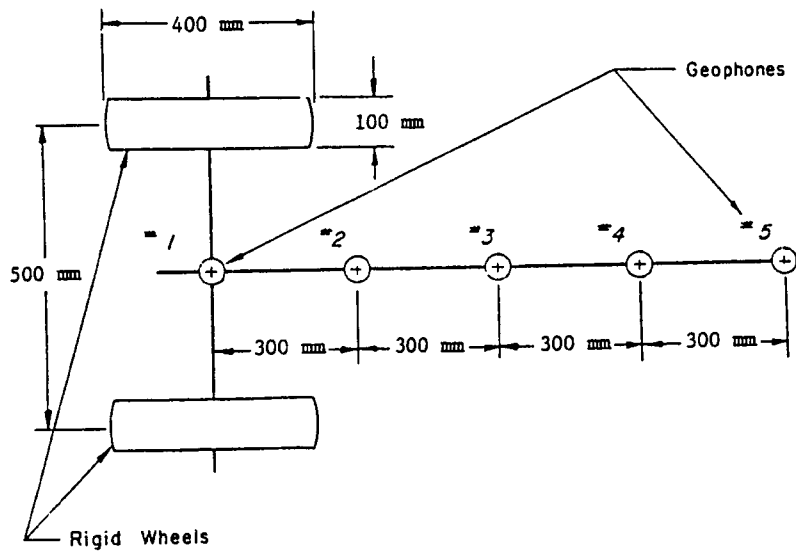


Figure 9. FWD impulse force traveling through deflection basin.

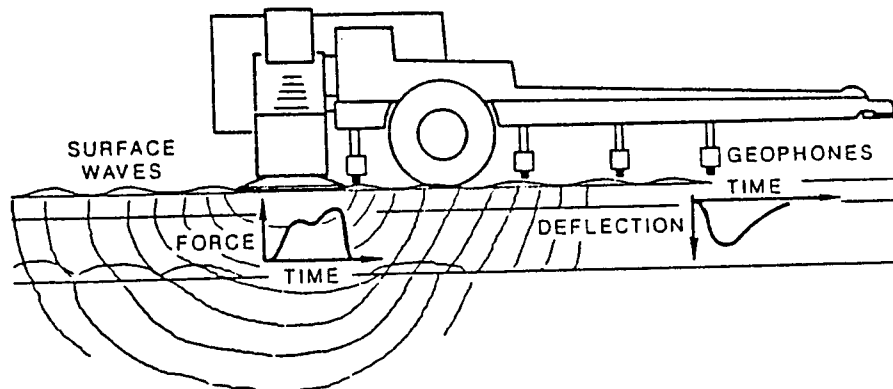


Figure 10. Sensors distributed uniformly (above) and nonuniformly (below).

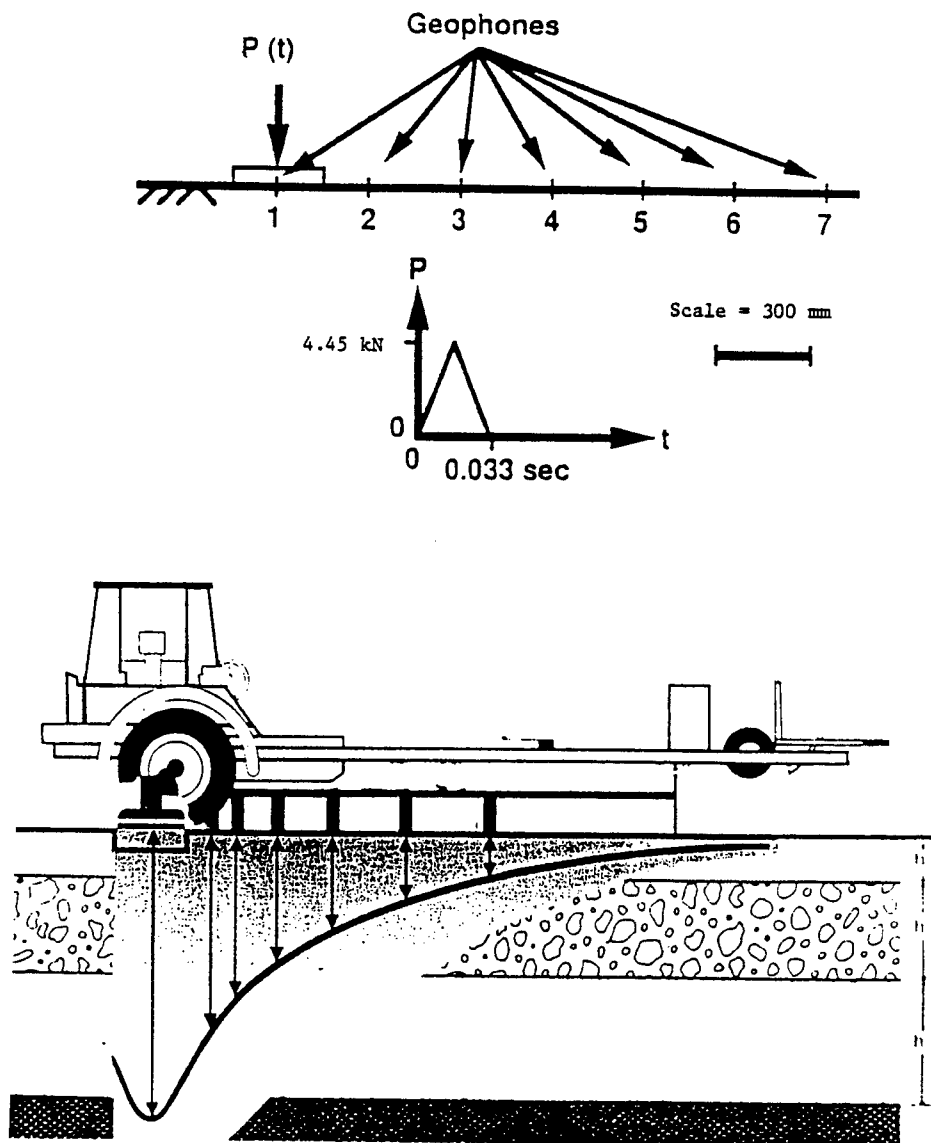


Figure 11. Measuring the deflection basin.

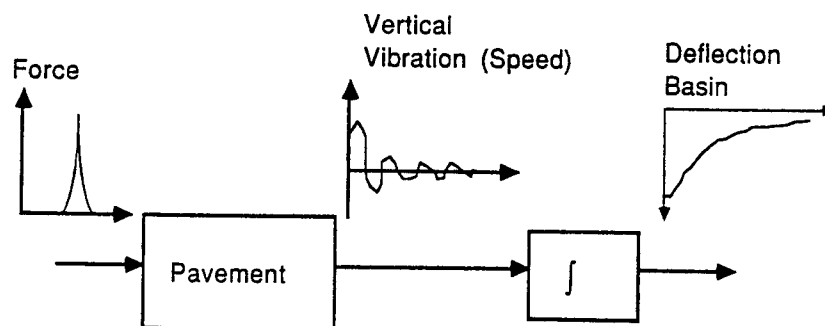




Figure 12. FWD conceptual hardware and software systems.

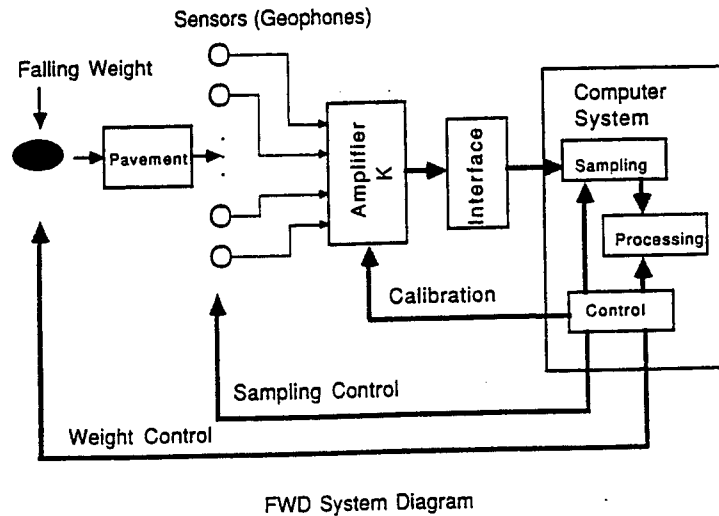


Table 1. Typical FWD specifications (KUAB model).

Specifications	2M-14	2M-23	2M-33	2M-44	2M-66
Load range (kips)	3-14	3-23	3-33	3-44	3-66
Load rise time (msec)	25	17/25	17/25	17/25	17/25
Load duration (msec)	50	34/50	34/50	34/50	34/50
Test times - standard 3 drop sequence (sec)	45	45	45	45	45
Sensor positions (inches)	0-120	0-120	0-120	0-120	0-120
Typical number of sensors	7-9	7-9	7-9	7-9	7-9
Sensor range (mils)	0-200	0-200	0-200	0-200	0-200
Segmented load plates (mm)	300	300/450	300/450	300/450	300/450

**Accuracy, Resolution and Repeatability**

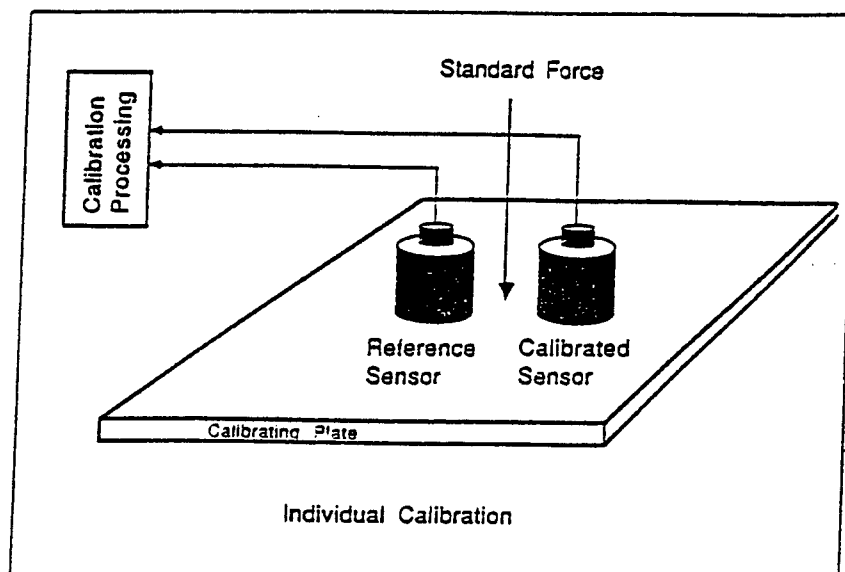
Seismometers	Absolute accuracy	Better than 2% of indicated reading + 2 microns (0.08 mils).
	Repeatability	Better than 0.5% of reading + 1 micron (0.04 mils).
	Resolution	Deflection readings down to 1 micron (0.04 mils).
Load Cell	Absolute accuracy	Better than 2% of the indicated rating.
	Resolution	8 pounds-force or better.

velocities at these points can be converted to deflections, and the deflection basin can be estimated. Figure 12 shows the FWD conceptual hardware and software systems, and Table 1 lists typical specifications.

E. FWD Calibration (The SHRP Procedure)

This includes individual and relative calibrations:

Figure 13. Individual calibration of FWD sensors.



1. The purpose of individual calibration is to determine the linear correlation model between the reference sensor and calibrated sensor, as shown in Figure 13. Each sensor should be calibrated, based on the reference sensor.
2. Relative calibration is used to determine the statistical difference between the calibrated sensor and a standard sensor. This is done to assure repeatability of measurement by any calibrated FWD.

Individual and relative calibrations should be conducted at specified time intervals to ensure that data collected are reliable. This calibration conforms to the procedure recommended by the Strategic Highway Research Program.

#### F. Further Research

The Engineering Research and Development Bureau is monitoring the Department's initial use of FWDs, focusing on three aspects -- evaluation, implementation, and application. This is based on analyses of correlation, repeatability, and environment. The major evaluation activity is collection of field and laboratory data. Implementation consists of training FWD users, preparing an operating

manual, and model development. During implementation, models will be developed predicting pavement responses and materials characteristics. The study will also collect information on such FWD applications as pavement evaluation and overlay design.

Table 2. Proposed parameters based on surface deflection\*.

Parameter	Formula <sup>a</sup>	Source
Radius of curvature <sup>b</sup>	$R = r^2/2d_0[(d_0/d_r) - 1]$	Miura and Tobe (18)
Deflection ratio <sup>c</sup>	$DR = d_r/d_0$	Claessen et al. (19)
Spreadability <sup>d</sup>	$SP = [(d_0 + d_1 + d_2)/3d_0] \times 100$	Rufford (20)
Bending index	$BI = d_0/a$	Hveem (21)
Radius of influence	$RI = R^1/d_0$	Ford and Bisselt (22)
Slope of deflection <sup>e</sup>	$SD = \tan^{-1}[(d_0 - d_r)/r]$	Kung (23)

<sup>a</sup> $r$  = radial distance from center of load;  $d$  = deflection (0 = center of load,  $r$  = radial distance, 1,2 = Locations 1 and 2;  $a$  = one-fourth length of deflection basin;  $R^1$  = distance from point of maximum deflection to where curve becomes tangent to horizontal.

<sup>b</sup> $r$  and radius for  $d_r = 127$  mm.

<sup>c</sup>Radius for  $d_r = 600$  mm.

<sup>d</sup> $d_1$  and  $d_2$  measured at 300 and 600 mm from the load, respectively.

<sup>e</sup> $r$  and radius for  $d_r = 610$  mm.

\*Adapted from Stock, A.F., and Yu, J. "Use of Surface Deflection for Pavement Design and Evaluation." Transportation Research Record 954, Transportation Research Board, 1984, pp. 64-69.

## MODULE IV: BACKCALCULATION OF MATERIAL PROPERTIES

### A. Deflection Data Analysis

To conduct an FWD test, a pulse load with a short loading time (about 28 milliseconds) is applied to the surface by a weight falling on a set of springs. The load is transferred to the pavement through a circular plate, and surface deflections are measured and recorded by seven geophones (sensors) at various distances from the loading point. Deflection-basin magnitude and shape are determined by characteristics of the pavement system, including layer thickness, Poisson's ratio, layer moduli, moduli ratio, and depth to the stiff layer (i.e., bedrock). To analyze surface deflection data, the following parameters can be used, where  $D_0$  = deflection at center of the loading plate and  $D_i$  = deflection at the sensor:

1. Maximum deflection  $D_0$ ,
2. Deflection basin area =  $6(1 + 2D_1/D_0 + 2D_2/D_0 + D_3/D_0)$ , and
3. Deflection shape factors  $F_1$  and  $F_2$ :  $F_1 = (D_0 - D_2)/D_1$ , and  $F_2 = (D_1 - D_3)/D_1$ .

In addition, other parameters have been proposed by researchers, as summarized in Table 2.

For a more sophisticated analysis, layer moduli can be "backcalculated" from the loads and surface deflection data, giving detailed information concerning material characteristics of each layer in the pavement system.

To compare relative changes of structural conditions between points (stations) and over time, the easiest and most convenient method is to plot surface deflection data. In general, the higher the deflection, the weaker the pavement system. "Outer" sensors typically register response of the deeper layers, and "inner" sensor deflection represents composite effects of whole pavement layers.

By plotting surface deflections over different time periods, one can visually examine changes in pavement structural conditions.

By computing deflections in the pavement system, a typical curve for 95 percent of surface deflection can be drawn (Fig. 14). It should be noted that depth beneath which 95 percent of surface deflection occurs declines gradually and moves downward with increasing radial distance from the loading plate. Actual shape and position of this curve are functions of the moduli and thicknesses of the pavement layers. However, one can say that most of the registered surface deflection is attributable to compression occurring in layers that are below the curve. Only a small portion (5 percent) of surface deflection occurs in materials above the curve. Thus, materials above it have almost no influence on measured surface deflection at any particular radial distance from the loading plate. This concept is used to interpret surface deflection data. Outer sensors characterize the deeper layers, and inner sensors represent composite effects of the pavement system. Sensor spacing for the layers is estimated with a 34-deg line, which provides a good estimation of the 95-percent deflection curve (Fig. 15).

As case studies, two asphalt-rubber test sites on New York State Rtes 17 and 144 were tested with FWDs in 1989 and 1992 (24). Four loads were applied and seven sensors -- positioned 0, 200, 325, 500, 800, 1250, and 1500 mm from the center of the loading plate -- recorded surface deflection. To examine pavement condition, surface deflections were plotted against station number. Data were normalized before plotting because most pavement design procedures use the 80-kN equivalent-single-axle-load (ESAL) concept (i.e., 40-kN per wheel load). In addition, it is known that pavement materials behave nonlinearly under loads (a nonlinear stress/strain relationship exists). Thus, among the four load levels, that closest to 40-kN was plotted.

Three sensors were used to represent response of three subsystems -- the entire pavement, the subbase and subgrade combined, and the subgrade alone. As mentioned earlier, a 34-deg line was used to estimate spacing for the layers, as shown in Figure 16. Center deflection ( $R = 0$ ) was used for all layers. The other two sensors were determined using  $R = \left[ \frac{\text{depth to top of layer}}{\tan(34 \text{ deg})} \right]$ . For Rte 17, sensor spacings of 0, 500, and 1250 mm were used, and for Rte 144, spacings of 0, 500, and 800 mm. Deflection data are plotted for Rtes 17 and 144 in Figures 17 and 18. By examining magnitude of deflection in micrometers, relative weakness and changes with time at each individual test station can be

Figure 14. Surface deflection.

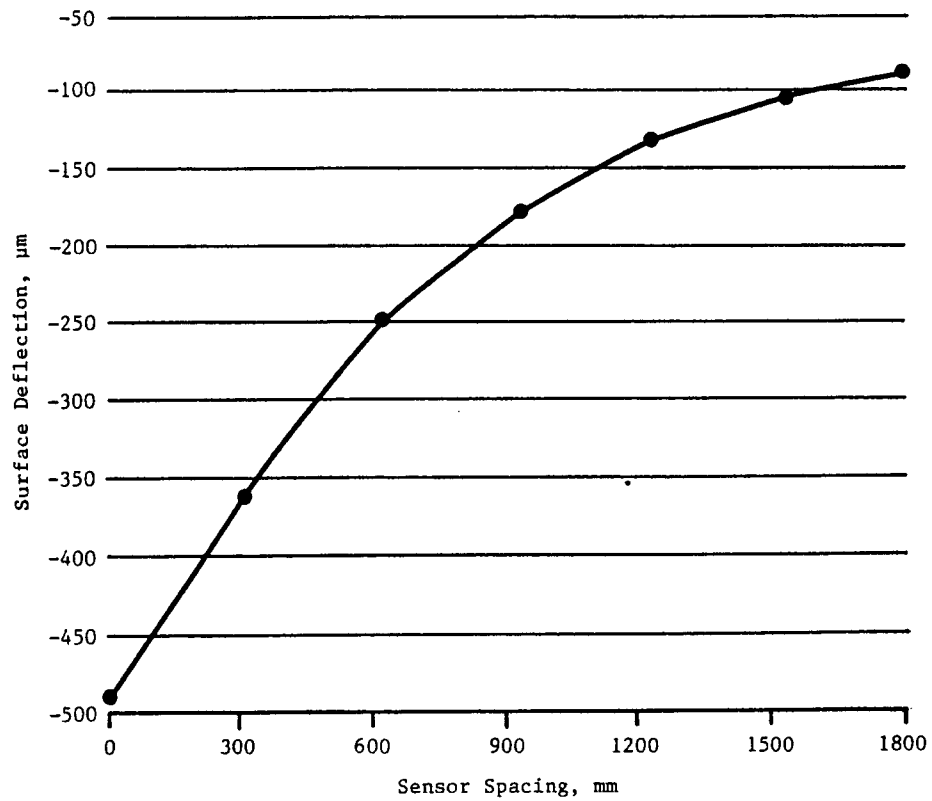


Figure 15. 95-percent deflection curve.

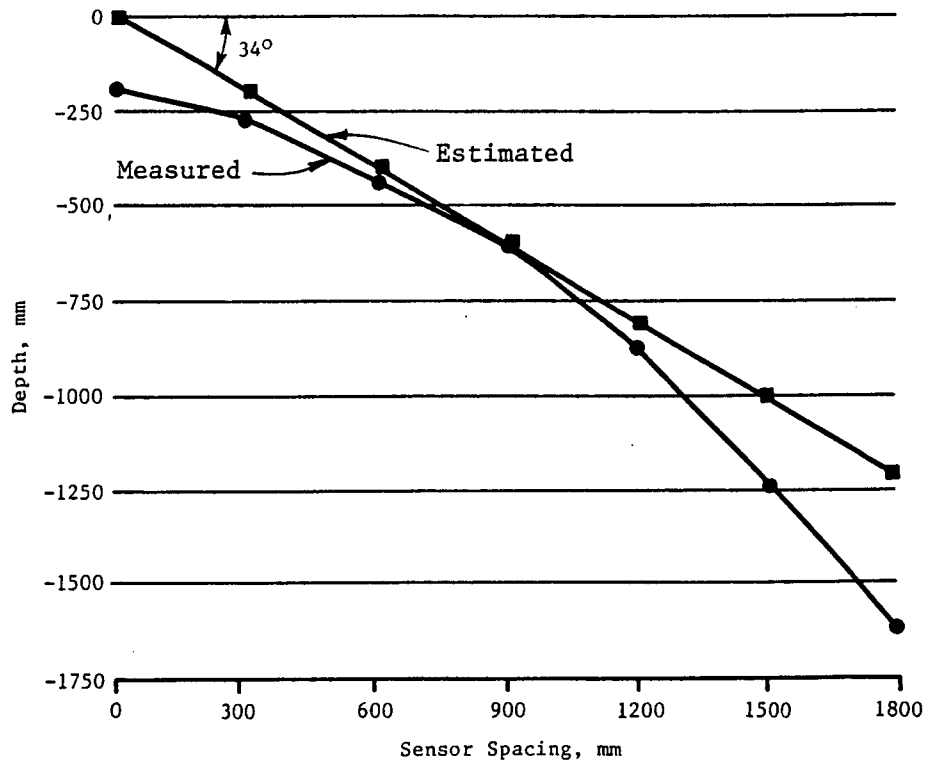
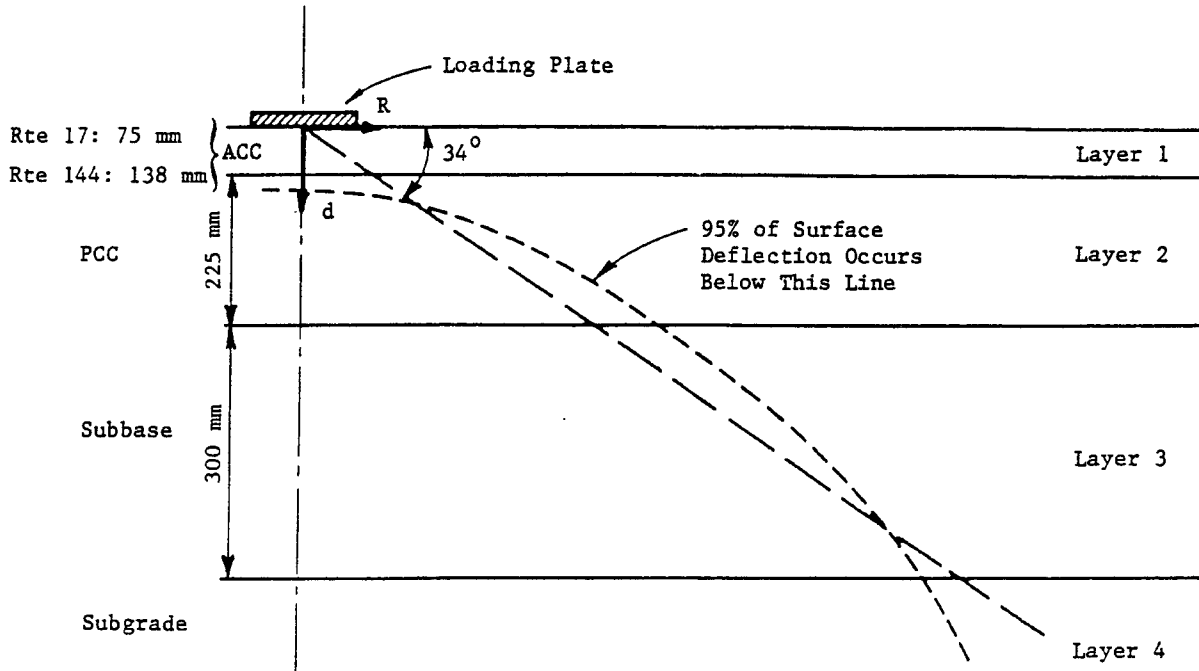


Figure 16. 95-percent deflection curves for Routes 17 and 144.



$$d/x = \tan (34^\circ)$$

$$x = d/\tan (34^\circ)$$

d = depth

x = horizontal distance from point of load application

R = actual distance from sensor to load point

	<u>Route 17</u>	<u>Route 144</u>
PCC & ACC Overlay:	d = 0 R = 0	d = 0 R = 0
Subbase:	d = 363 mm	d = 300mm
	$x = \frac{363 \text{ mm}}{\tan (34^\circ)} \approx 538 \text{ mm}$ R = 500mm	$x = \frac{300 \text{ mm}}{\tan (34^\circ)} \approx 448 \text{ mm}$ R = 500mm
Subgrade:	d = 600mm	d = 600mm
	$x = \frac{600 \text{ mm}}{\tan (34^\circ)} \approx 889.5 \text{ mm}$ R = 800mm	$x = \frac{600 \text{ mm}}{\tan (34^\circ)} \approx 889.5 \text{ mm}$ R = 800mm



Figure 17. Rte 17 driving lane normalized deflections summarized by date.

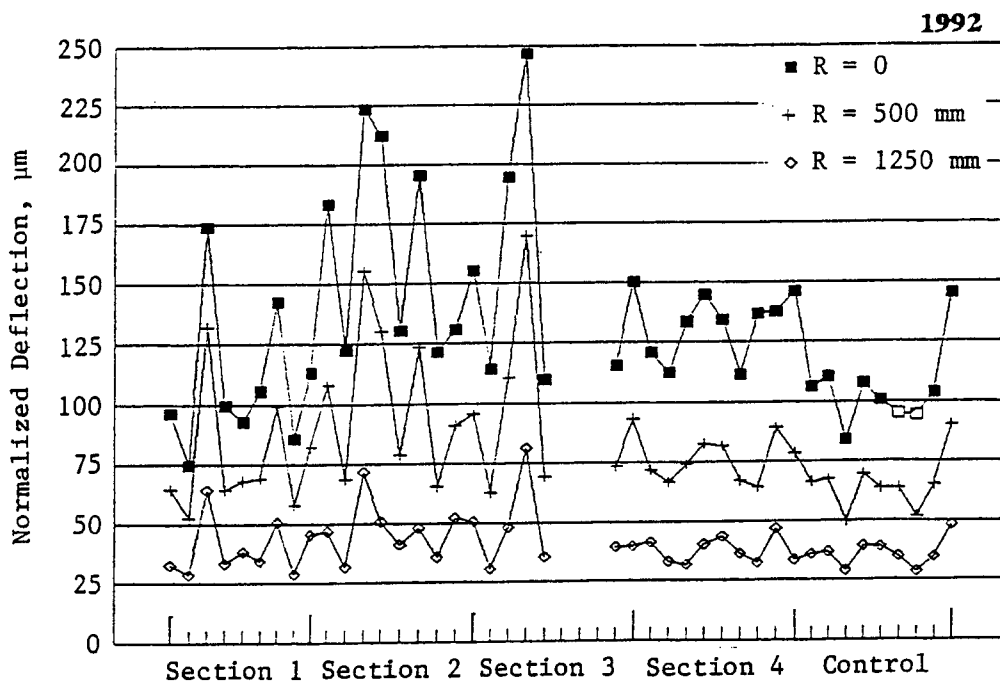
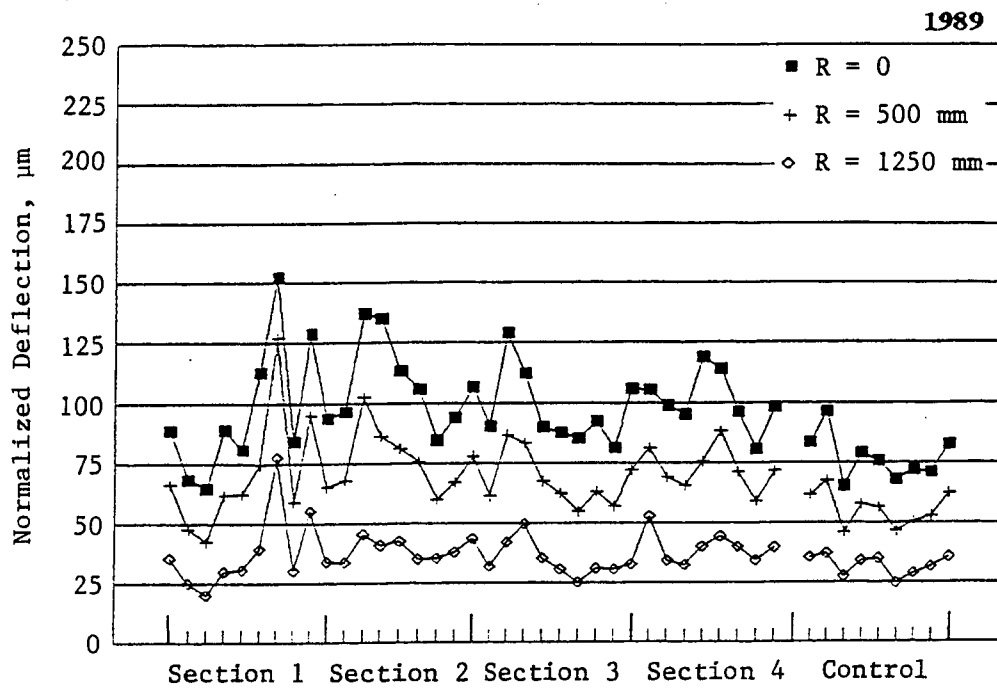
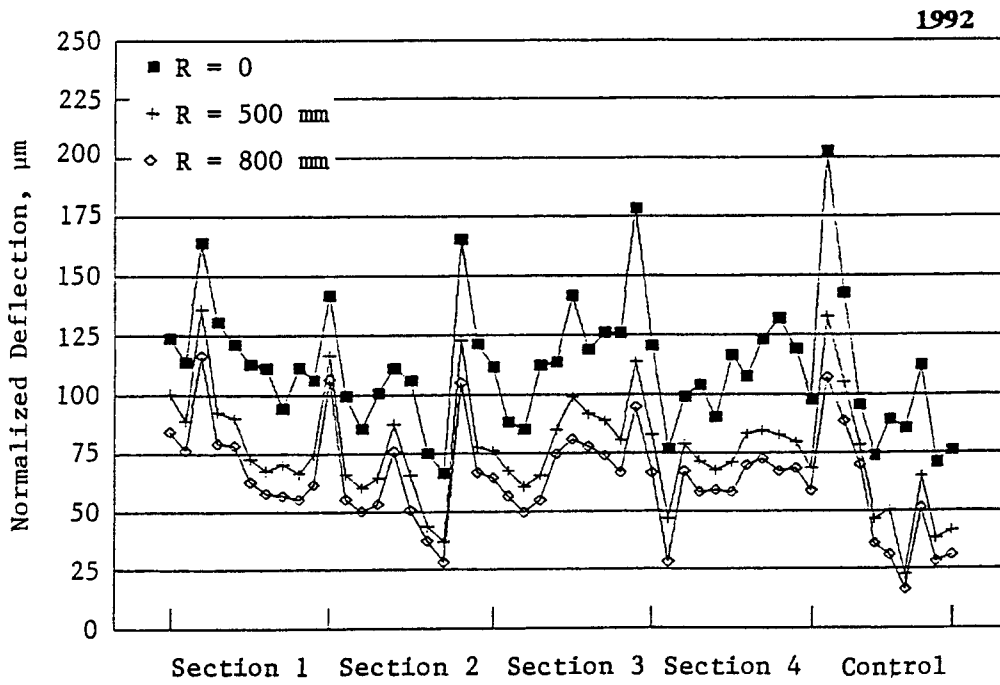
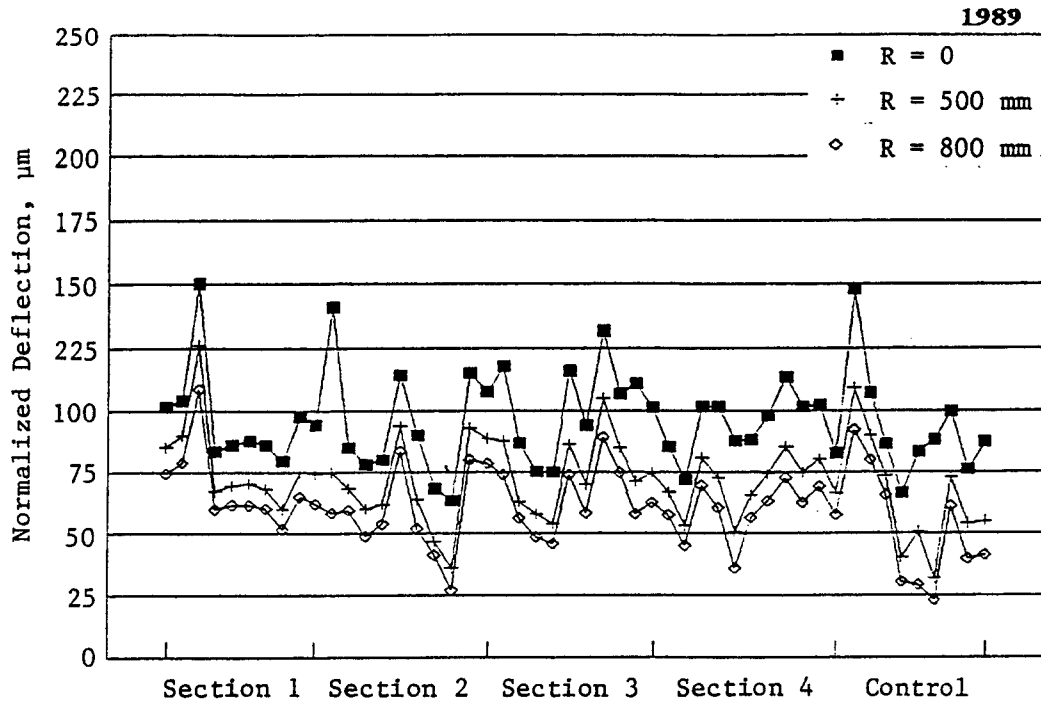


Figure 18. Rte 144 driving lane normalized deflections summarized by date.



identified, as well as layer(s) responsible for any weaknesses. Some general statements can be made regarding analysis of the FWD test results:

Rte 17

1. In Figure 17 it can be noted that center deflections increased from 1989 to 1992. Thus, overlays in all sections have deteriorated.
2. Comparing deflections at  $R = 500$  in Figure 17, the subbase beneath Section 4 and the control section remained essentially the same, since their deflections were both about  $75 \mu\text{m}$ . Four points appear to have weakened from 1989 to 1992 -- one in Section 1, one in Section 3, and two in Section 2 -- with relatively high increases in the readings at  $R = 500$ .
3. It can be observed in the 1992 plot that subbase condition for Section 4 and the control section is relatively better than for the other three sections, with deflection at  $R = 500$  smaller and more uniform than in the other three sections. Some of this variation in the Sections 1, 2, and 3 can be attributed to the subgrade, since it exhibits the same pattern.
4. Comparing 1989 and 1992 deflection readings at  $R = 1250$ , the subgrade remained fairly constant except for one reading around  $50 \mu\text{m}$  each in Sections 1, 2, and 3.
5. From the 1992 graph in Figure 17, the section in best overall condition was the control (with smallest deflections) and the poorest were Sections 2 and 3 (with highest deflections).

Rte 144

1. From Figure 18 most of the control section's subbase and subgrade are registering low deflections ( $R = 500$  and  $800$ , respectively), with the other sections performing adequately, as before.
2. Each section has at least one station exhibiting relatively significant high-deflection readings at all three sensors, with Section 3 the worst. Since all three sensors exhibited the same high reading, the weakness is probably attributable to the subgrade.

3. The increase in deflection readings at R = 800 from 1989 to 1992 means the subgrade has deteriorated in strength, but the subbase had remained essentially the same.
4. From the 1992 data, in terms of overall pavement performance, the control section is performing best of all layers because it exhibits lowest deflections. Seasonal variations were not considered in this analysis.

## B. Programs for Backcalculation

### 1. The MODCOMP Program

The computer program MODCOMP 3 was developed at Cornell University by Irwin (25) to interpret moduli of elasticity of pavement layers from surface deflection data. It uses an iterative approach where layer moduli are systematically varied until a fit of surface deflection data is achieved.

MODCOMP 3 can handle data from up to ten deflection sensors at up to six load levels. The pavement system may have up to twelve layers, although it is recommended that no more than five or six have unknown moduli.

It is important to understand that certain pavement features affect surface deflections, but others have little influence. In general, backcalculation can determine moduli only for pavement layers that significantly influence surface deflection.

Pavement surface deflections are relatively insensitive to monitored variations in pavement moduli; this results in backcalculation of pavement layer moduli being highly sensitive to minor variations (or errors) in measured surface deflections. Deflection errors on the order of only 1 or 2  $\mu\text{m}$  will dramatically affect the resultant moduli. Thus, for best results with backcalculation, it is essential to use data from a calibrated nondestructive-testing device.

To determine unknown layer moduli, surface deflections must be associated with the pavement layers. MODCOMP 3 can use its own logic to make the assignments, or the user may make them. There is a limit, however, as to how deep a layer with an unknown modulus can be positioned. MODCOMP 3 generally can determine moduli for layers lying at a depth no more than the radial distance from the

center of load to the outermost deflection sensor. If the layer is so deep that it has little or no influence on the outermost deflection, then its modulus cannot be determined accurately.

In addition to knowing deflections and loading conditions, one must also know pavement layer thickness and a value for Poisson's ratio for each layer. Accurate knowledge of layer thickness is important, since computational results are sensitive to thickness. Layer thickness should be known to a degree of precision of 5 percent or more.

There is no closed-form solution in determining layer moduli from surface deflection data, so an iterative approach is used in the computations. The basic principle is to begin with a user-supplied set of "seed" moduli, from which surface deflections are computed using the Chevron program (6). Computed deflections are compared to measured deflections, and seed moduli are adjusted as a function of magnitude of the difference in deflections. Then a layer modulus is interpolated to agree with the measured deflection.

The process is repeated for each layer until agreement between calculated and measured deflections is within the specified tolerance, or until the allowed number of iterations has been exhausted.

The program first evaluates the modulus of the deepest unknown layer, and then works upward to the surface layer. Measured deflections at greater radii are assigned to deeper layers. Thus as the program works upward from the deeper layers, it also works inward toward the center of the deflection basin.

Detailed information regarding the MODCOMP 3 program can be found in its user's guide (25).

## 2. The MODULUS Program

This backcalculation program was developed in Texas by Uzan (26). This is a microcomputer-based program and can be used in two-, three-, four-, or five-layer pavement systems. MODULUS 4.0 uses the Corps of Engineers WES5 linear elastic program, which is considerably faster than many other existing programs and has no copyright restrictions. It also has the following added features:

1. Automatic calculation of depth to a stiff layer, which the user can override.

2. Automatic calculation of weighted factors for each layer.
3. Detection of nonlinearity in the subgrade, and automatic selection of optimum numbers of sensors to use in backcalculation.

The MODULUS program was developed to estimate pavement material properties from nondestructive testing. The procedure is to find the set of parameters corresponding to the best fit of the measured deflection basins. Best fit is achieved by minimizing the error between measured and calculated surface deflection basins. Thus, the following equation is to be minimized:

$$\epsilon^2 = \sum_{i=1}^s \left[ \frac{W_i^m - W_i^c}{W_i^m} \right]^2 W_{e_i} \quad (28)$$

where  $\epsilon^2$  = squared error,

$W_i^m$  = measured deflection at Sensor  $i$ ,

$W_i^c$  = computed deflection at Sensor  $i$ ,

$s$  = number of sensors, and

$W_{e_i}$  = a user-supplied weighing factor for Sensor  $i$ .

To minimize Eq. 28, MODULUS uses the Hooke-Jeeves pattern-search algorithm, which provides a definite convergence. MODULUS has the following advantages:

1. Once the deflection basin's database is calculated, the process requires little time to complete; this is an excellent tool for routine analysis of a known pavement system.
2. Estimation of stiff layers and weighting factors is provided.

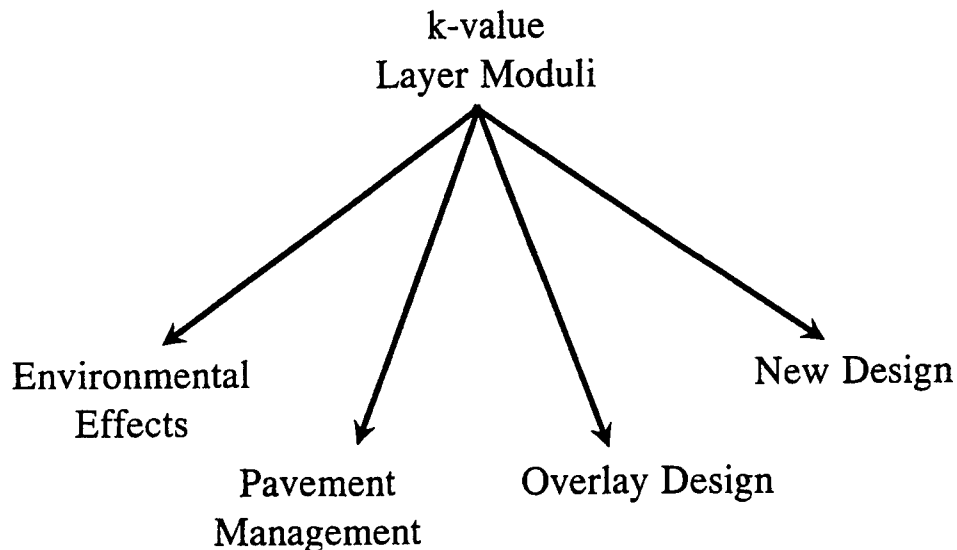
## MODULE V: APPLICATIONS OF THE FALLING-WEIGHT DEFLECTOMETER

The FWD allows backcalculation of layer material properties, specifically the k- and E-values for various layers. These have several applications (Fig. 19). Layer moduli can be backcalculated using several different procedures, which fall into three basic categories: 1) layered-elastic systems, 2) database comparison, and 3) nomographs.

Layered-elastic systems use mathematical models to calculate pavement response under surface loads for various pavement properties. An iterative process is then used to bring measured and theoretical deflections into agreement. Numerous backcalculation programs are currently available. The main drawback to the iterative layered-elastic procedure is that it is relatively slow compared to the comparative procedure.

The comparative procedure begins by storing many deflection basins and their corresponding layer moduli in a database. Next, the measured deflection basin is compared with those in the database to find the closest match. Layer moduli

Figure 19. Applications of the falling-weight deflectometer.



are then taken as those corresponding to the match. By eliminating the iterative process, the database approach has increased the speed of backcalculation. Two database programs available are MODULUS (26) and COMPDEF (27).

The third method uses nomographs to obtain layer moduli. To develop a nomograph, deflection basins for different layer moduli are generated using layered-elastic programs. Maximum deflection or basin area is then graphically related to various layer moduli. (This is the least popular of the three procedures.)

#### A. Benefits for Pavement Management Systems

The FWD provides a method for rapid inventory of many miles of pavement. An extensive study of 15 deflection devices (28) ranked the FWD best for both project- and network-level pavement evaluation. The FWD provides a relatively inexpensive method for rapid testing, and the test is performed in an undisturbed state. Layer properties can be used to determine structural capacity, which can then be applied in a pavement evaluation program. A survey of existing pavements provides a catalog of current pavement conditions, allowing continuing evaluation of design procedures, and helps in determining deficiencies of the current design procedure. Pavement conditions can then be related to requirements for routine or major maintenance, rehabilitation, and reconstruction. This information also provides a basis for extended planning of expenditures.

#### B. Design Procedures

Overlay design may be developed by three methods:

1. Using the FWD or another nondestructive testing device to estimate material properties on which to base a mechanistic-empirical design.
2. Estimating the variables needed for overlay design based on a pavement condition survey (low-volume roads only).
3. Using lab tests to estimate in-situ material properties.

The FWD can provide data necessary to use mechanistic-empirical design procedures for both new pavements and overlays. The one constraint is that the method used for design should be the same as for backcalculation of FWD deflection data -- i.e., if layered-elastic theory is to be used in the design process, it should



also be used for backcalculating moduli. Furthermore, assumptions used in backcalculation should be consistent with those for design. For new pavements, it is suggested that FWD tests be performed on existing pavements near the new design location, with similar soil types.

The FWD can also be used to determine structural condition of existing pavements based on deflections. Deflection data can then help determine layer moduli. An example of using FWD measurements to design overlays is the revised AASHTO overlay design manual (29), which will now be discussed.

### 1. Bituminous Overlays on Flexible Pavements

AASHTO overlay design includes the following steps:

1. Determining existing pavement design and construction parameters.
2. Traffic analyses (past and future).
3. Condition surveys.
4. Deflection testing (optional, but strongly recommended).
5. Coring and materials testing (optional, but strongly recommended).
6. Determining required structural number for future traffic.
7. Determining effective structural number ( $SN_{eff}$ ) of existing pavement.
8. Determining overlay thickness.

#### Step 1: Determining Existing Pavement Design and Construction Parameters

Determine thickness, material type, and subgrade soil data from construction records, soil surveys, county agricultural reports, etc.

#### Step 2: Traffic Analyses

Determine cumulative ESALs for the design lane from opening to date and from now to the end of overlay design life.

Step 3: Condition Surveys

Determine distress types and severities for the most heavily traveled lane. The following should result from the condition survey:

1. Percent of surface area with alligator cracking.
2. Number of transverse cracks per mile.
3. Mean rut depth.
4. Evidence of pumping at cracks and pavement edges.

Note that Categories 1 and 2 should be subdivided into low-, medium-, and high-severity cracking.

Step 4: Deflection Testing

Measure deflections in the wheelpaths to assess condition of the existing pavement. It is recommended that an FWD be used, with a 40-kN load magnitude and a test interval of 30 to 300 m. (For further guidance, AASHTO refers to ASTM Methods D 4694 and D 4695.) From deflection testing, the following methods are suggested for determination of subgrade resilient modulus  $M_r$ , and effective modulus for the pavement  $E_p$ .

The  $M_r$  value is determined using this equation:

$$M_r = \frac{0.24P}{d_r r} \quad (29)$$

where  $M_r$  = backcalculated subgrade resilient modulus, MPa,

$P$  = applied load, N,

$d_r$  = deflection at distance  $r$  from center of load, mm, and

$r$  = distance from center of load, mm.

Note that no temperature adjustment is needed since  $M_r$  is based on only subgrade deflection. AASHTO also provides Eq. 30 for determining  $E_p$ , based on deflection at the center of the load plate:

$$d_0 = 1.5 pa \left[ \frac{1}{M_r \sqrt{1 + \left( \frac{D}{a} \sqrt[3]{\frac{E_p}{M_r}} \right)^2}} + \left[ \frac{1 - \frac{1}{\sqrt{1 + \left( \frac{D}{a} \right)^2}}}{E_p} \right] \right] \quad (30)$$

where  $d_0$  = deflection (mm) measured at center of load plate (and adjusted to a standard temperature of 20°C),

$p$  = nondestructive-testing load-plate pressure, MPa,

$a$  = nondestructive-testing load-plate radius, mm,

$D$  = total thickness of pavement layers, mm,

$M_r$  = subgrade resilient modulus, MPa, and

$E_p$  = effective modulus of all pavement layers above subgrade, MPa.

The deflection used to determine  $M_r$  must be measured far enough away that it provides a good estimate of  $M_r$  independent of effects of any layers above, but close enough that it can be measured accurately. AASHTO provides the following relationship for determining minimum distance ( $r$ ):

$$r \geq 0.7 a_e \quad (31a)$$

and

$$a_e = \sqrt{a^2 + \left( D \sqrt[3]{\frac{E_p}{M_r}} \right)^2} \quad (31b)$$

where  $a_e$  = radius of the stress bulb at the subgrade-pavement interface, mm,

- a = nondestructive-testing load-plate radius, mm,
- D = total thickness of pavement layers above subgrade, mm, and
- $E_p$  = effective modulus of all pavement layers above subgrade, MPa.

#### Step 5: Coring and Materials Testing

Although not mandatory, this step is strongly recommended to determine thicknesses and condition of existing pavement layers. Coring and materials testing should determine the following:

1. Resilient modulus of subgrade (if FWD testing is not performed).
2. Asphalt concrete layers and the stabilized base should be sampled for evidence of asphalt stripping, degradation, and erosion.
3. The base and subbase should be sampled and gradations run to determine degree of degradation and contamination by fines.
4. Thickness of all layers should be measured.

#### Step 6: Determining Structural Number for Future Traffic ( $SN_f$ ).

Use the design  $M_r$  value as a parameter to determine the required  $SN_f$ . The design  $M_r$  (in MPa) for a FWD is determined using the following equation:

$$\text{Design } M_r = C \left( \frac{0.24p}{d_r r} \right) \quad (32)$$

where C = a correction factor, necessary to make  $M_r$  consistent with the laboratory-measured value used for the AASHO Road Test soil in developing the design equation,

- $d_r$  = deflection at r, mm,
- r = distance from center of load plate, mm, and
- p = load, N.

AASHTO recommends  $C = 0.33$  when using an FWD load of about 40 kN. Next, the structural number needed to carry future traffic ( $SN_f$ ) is computed using the design  $M_r$  (Eq. 32) just calculated in the flexible pavement design equation.

Step 7: Determining Effective Structural Number ( $SN_{eff}$ )

Determine this number for the existing pavement as follows:

$$SN_{eff} = 0.00093 D \sqrt[3]{E_p} \quad (33)$$

where  $D$  = total thickness of all pavement layers above the subgrade, mm, and

$E_p$  = effective modulus of pavement layers above the subgrade, MPa.

If deflection testing is not used, then  $SN_{eff}$  must be estimated based on a condition survey.

Step 8: Determining Overlay Thickness ( $D_{ol}$ )

Find this as follows:

$$D_{ol} = \frac{SN_{ol}}{a_{ol}} \times 25 \quad (34)$$

$$D_{ol} = \frac{(SN_f - SN_{eff})}{a_{ol}} \times 25$$

where  $SN_{ol}$  = required overlay structural number,

$a_{ol}$  = structural coefficient for the overlay,

$D_{ol}$  = required overlay thickness, mm,

$SN_f$  = structural number found in Step 6, and

$SN_{eff}$  = effective structural number of the existing pavement (from Step 7).

## 2. Bituminous Overlays on Rigid Pavements

AASHTO design of bituminous overlays requires the following steps:

1. Determining existing pavement design parameters.
2. Traffic analyses.
3. Condition surveys.
4. Deflection testing (optional, but strongly recommended).
5. Coring and materials testing (optional, but strongly recommended).
6. Determining required slab thickness for future traffic ( $D_f$ ).
7. Determining effective slab thickness of existing pavement ( $D_{eff}$ ).
8. Determining overlay thickness.

### Step 1: Existing Pavement Design Parameters

Determine existing slab thickness, load-transfer type, and shoulder type by examining the pavement or construction records.

### Step 2: Traffic Analysis

Same as for bituminous overlays on flexible pavements.

### Step 3: Condition Surveys

Same as for bituminous overlays on flexible pavements.

### Step 4: Deflection Testing

The suggested procedure starts with measuring basins at intervals of 30 to 300 m (the exact interval should be sufficient to assess conditions adequately). The AASHTO method requires locating sensors at 0, 300, 600, and 900 mm from the center of the load, and recommends a load magnitude of 40 kN. The overlay design manual (29) also provides nomographs (Figs. 20

and 21) for determining effective k-value and the slab's elastic modulus. The nomographs require computation of deflection basin area, as follows:

$$\text{AREA} = 6 \left[ 1 + 2 \left( \frac{d_{300}}{d_0} \right) + 2 \left( \frac{d_{600}}{d_0} \right) + \left( \frac{d_{900}}{d_0} \right) \right] \quad (35)$$

where  $d_0$  = deflection at the center of the loading plate, mm, and

$d_1$  = deflection (mm) at 300, 600, and 900 mm from the plate's center.

1. Using area of deflection basins and the nomographs, determine the dynamic k-value using Figure 20.
2. Determine effective static k-value (half the effective dynamic k-value).
3. Entering Figure 21 with the effective dynamic k-value, and area of the deflection basin, solve for  $ED^3$ , where D is slab thickness. Solve for E (in MPa), knowing the slab thickness D (in mm).
4. Determine joint load transfer by placing the load plate on one side of the joint with its edge touching the joint, and measuring deflection at the center of the load plate and 300 mm from the center (on the unloaded slab). Deflection load transfer can then be computed as follows:

$$\Delta \text{LT} = 100 \left( \frac{\Delta_{ul}}{\Delta_1} \right) B \quad (36)$$

where  $\Delta \text{LT}$  = deflection load transfer, percent,

$\Delta_{ul}$  = unloaded-side deflection, mm,

$\Delta_1$  = loaded-side deflection, mm, and

B = slab bending correction factor (this value is the ratio of  $d_0$  to  $d_{12}$  from a center-slab deflection test; typical values are from 1.05 to 1.15). (This slab bending

Figure 20. Effective dynamic k-value determination from  $D_0$  and AREA [Fig. 14.2 from the 1993 AASHTO Guide for Design of Pavement Structures (29)]. (1 pci = 0.27 MPa/m, 1 lb = 4.45 N, 1 in. = 25 mm, 1 mil = 25 microns)

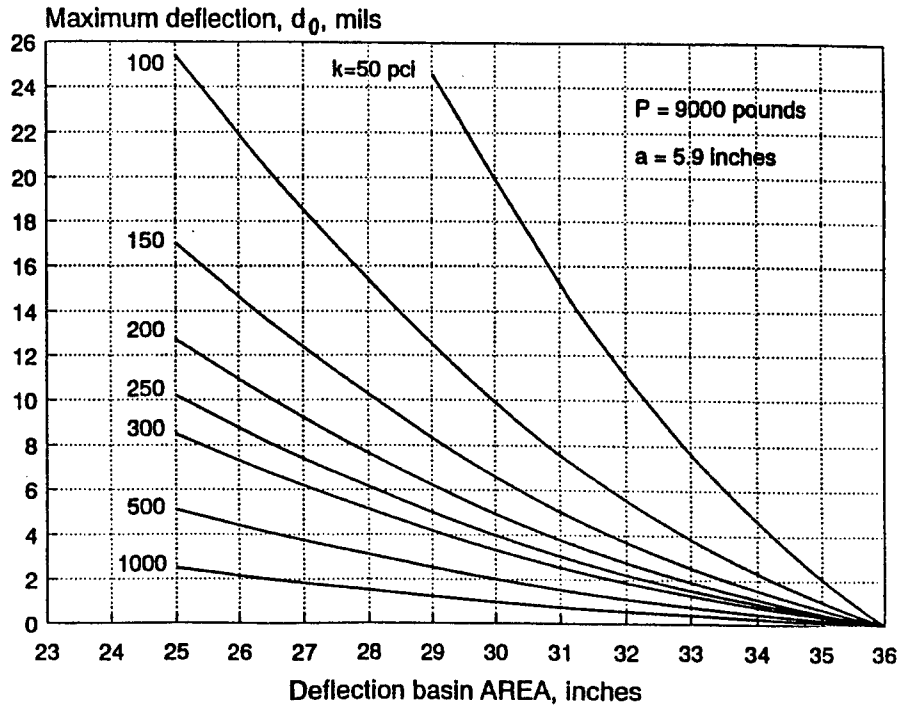
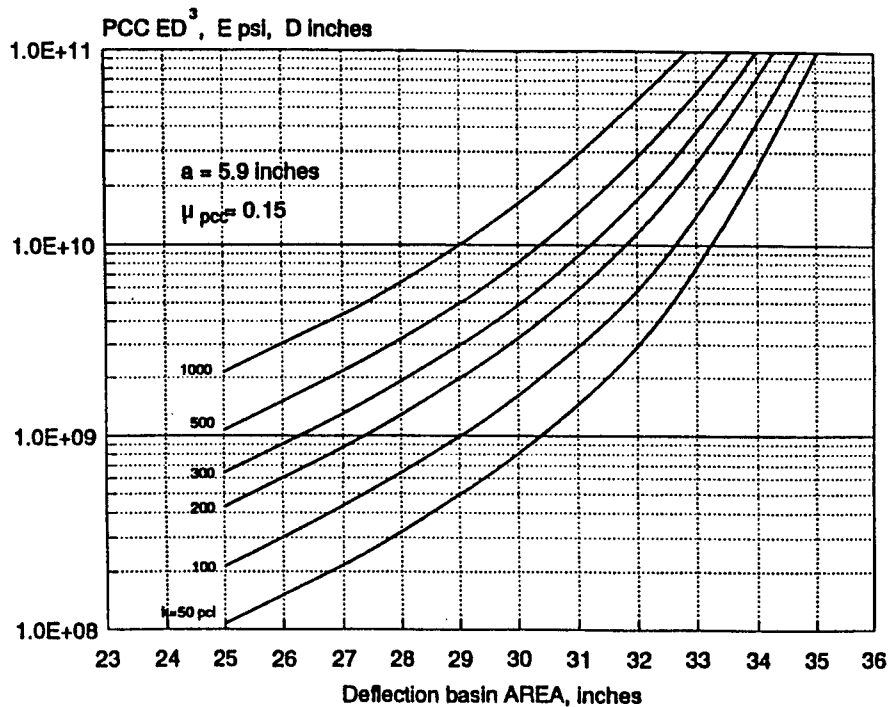


Figure 21. Concrete elastic modulus determination from k-value, AREA, and slab thickness [Fig. 14.3 from the 1993 AASHTO Guide for Design of Pavement Structures (29)]. (1 in. = 25 mm, 1 MPa = 0.145 ksi)





correction factor is necessary because deflections at 0 and 300 mm would not be equal, even if measured at the interior of the slab.)

The J load-transfer coefficient is then determined as follows:

Percent Load Transfer	J
>70	3.2
50-70	3.5
<50	4.0

#### Step 5: Coring and Materials Testing

From 150-mm diam cores from the center of the slab and indirect tensile tests, determine the concrete modulus of rupture.

#### Step 6: Determining Required Slab Thickness for Future Traffic ( $D_f$ )

Using the AASHTO design equation, nomograph, or DARWin program (30), determine slab thickness necessary to carry traffic from the present to some point in the future.

#### Step 7: Determining Effective Slab Thickness ( $D_{eff}$ ) of Existing Pavement

AASHTO provides two methods, the first based on condition surveys and the second on remaining life (RL). The procedure for determining  $D_{eff}$  from RL is as follows:

1. Compute RL as follows:

$$RL = 100 \left[ 1 - \left( \frac{N_p}{n_{1.5}} \right) \right] \quad (37)$$

where RL = remaining life, percent,

$N_p$  = total traffic to date, ESALs, and

$N_{1.5}$  = total traffic (ESALs) to pavement "failure" ( $N_{1.5}$  may be estimated using the AASHTO rigid pavement design equations, nomographs, or the DARWin program, a "failure" PSI of 1.5, and reliability of 50 percent).

2. Determine condition factor (CF) using RL and Figure 22 in the revised AASHTO overlay design manual.
3. Calculate  $D_{\text{eff}}$  as follows:

$$D_{\text{eff}} = \text{CF} \times D \quad (38)$$

where CF = control factor, and

D = thickness of the existing slab, mm.

#### Step 8: Determining Overlay Thickness

Bituminous overlay thickness is computed as follows:

$$D_{\text{ol}} = A(D_f - D_{\text{eff}}) \quad (39)$$

where  $D_{\text{ol}}$  = required thickness of bituminous overlay, mm,

A = a factor to convert rigid pavement thickness deficiency to bituminous overlay thickness,

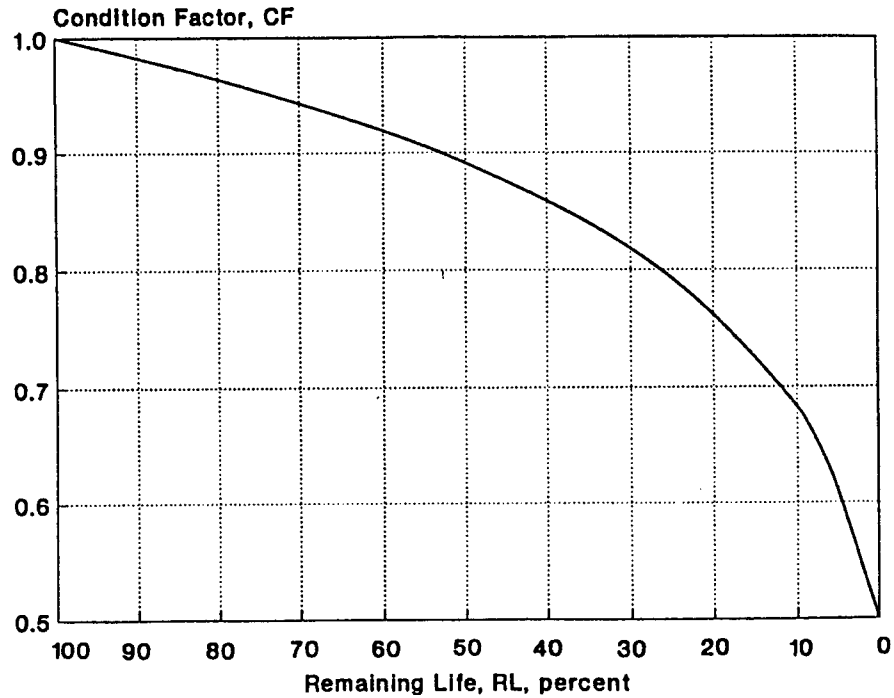
$D_f$  = slab thickness (mm) determined in Step 6, and

$D_{\text{eff}}$  = effective thickness (mm) of the existing slab determined in Step 7.

The A factor is a function of rigid pavement thickness deficiency, and is calculated as follows:

$$A = 2.2233 + 0.0099 (D_f - D_{\text{eff}})^2 - 0.1534 (D_f - D_{\text{eff}}) \quad (40)$$

Figure 22. Relationship of condition factor and remaining life [Fig 15.1 from the 1993 AASHTO Guide for Design of Pavement Structures (29)].



### C. Other Uses

The FWD can be used to determine the effect of seasonal variations on structural capacity of pavements. Alaska (31) has used the FWD to determine damage potential during spring thaw, and has modified load restrictions during such periods based on FWD data.



## REFERENCES

1. Boussinesq, J. Application des Potentials à l'Étude de l'Equivaliars et du Mouvement des Solides Elastiques. Paris: Gauthier-Villars, 1895.
2. Burmister, D. M. "The Theory of Stresses and Displacements in Layered Systems and Applications to the Design of Airport Runways." Proceedings, Highway Research Board, Vol. 23 (1943), pp. 126-48.
3. Acum, W. E. A., and Fox, L. "Computation of Load Stresses in a Three-Layer Elastic System." Geotechnique, Vol. 2 (1951), pp. 293-300.
4. Mehta, R. R., and Veletsos, A. S. Stresses and Displacements in Layered Systems. Structural Research Series 178, Civil Engineering Studies, University of Illinois (Urbana), 1959.
5. Michelow, J. Analysis of Stresses and Displacements in an N-Layered Elastic System Under a Load Uniformly Distributed on a Circular Area. Richmond, CA: California Research Corporation, 1963.
6. Thickness Design: Asphalt Pavements for Highways and Streets. Manual Series No. 1 (MS-1), Asphalt Institute, February 1991.
7. Schiffman, R. L. "General Analysis of Stresses and Displacements in Layered Elastic Systems." Proceedings, First International Conference on Structural Design of Asphalt Pavements, Ann Arbor, MI, 1962, pp. 365-75.
8. SHELL Pavement Design Manual. London: Shell International Petroleum Company, Ltd., 1978.
9. Winkler, E. Die Lehre von der Elasticitat und Festigkeit. Prage: Dominicus, 1867.

10. Yoder, E. J., and Witczak, M. W. Principles of Pavement Design. New York: John Wiley and Sons, 1975 (2nd ed.).
11. Tabatabaie-Rissi, A. M. Structural Analysis of Concrete Pavement Joints. Ph.D. Thesis, University of Illinois (Urbana), 1977.
12. The AASHO Road Test. Special Reports 61A through 61F, Highway Research Board 1961.
13. AASHTO Guide for Design of Pavement Structures: 1986. Washington: American Association of State Highway and Transportation Officials, 1986.
14. Friberg, B. F. "Design of Dowels in Transverse Joints of Concrete Pavements." Transactions of the American Society of Civil Engineers, Vol. 105, 1940, pp. 1076-95.
15. Tabatabaie, A. N., Barenberg, E. J., and Smith, R. E. Longitudinal Joint Systems in Slip-Formed Rigid Pavements: Vol. II, Analysis of Load Transfer Systems for Concrete Pavements. Research Report FAA-RD-79-4, II, Federal Aviation Administration, 1979.
16. Smith, K. D., Peshkin, D. G., Darter, M. I., Mueller, A. L., and Carpenter, S. H. Performance of Jointed Concrete Pavements: Vols. I through VI. Reports FHWA-RD-136 through -141, Federal Highway Administration, U. S. Department of Transportation, 1990.
17. Darter, M. I., Becker, J. M., Snyder, M. B., and Smith, P. E. Portland Cement Concrete Pavement Evaluation System (COPES). Report 177, National Cooperative Highway Research Program, Transportation Research Board, 1985.
18. Miura, Y. and Tobe, R. "Evaluation of Existing Pavements Based on Deflection and Radius of Curvature and Overlay Design." Proceedings, Fourth International Conference on the Structural Design of Asphalt Pavements, Ann Arbor, MI, 1977, pp. 862-75.
19. Claessen, A. I. M., Valkering, C. P., and Ditmarsch, R. "Pavement Evaluation with the Falling Weight Deflectometer." Proceedings, Association of Asphalt Paving Technologies, Vol. 45 (1976), pp. 122-57.

20. Rufford, P. G. "A Pavement Analysis and Structural Design Procedure Based on Deflection. Proceedings, Fourth International Conference on the Structural Design of Asphalt Pavements, Ann Arbor, MI, 1967, pp. 710-21.
21. Hveem, F. N. "Pavement Deflection and Fatigue Failures." Bulletin 114, Highway Research Board, 1955, pp. 43-73.
22. Ford, J. C., Jr., and Bisselt, J. R. "Flexible Pavement Performance Studies in Arkansas." Bulletin 321, Highway Research Board, 1962, pp. 1-15.
23. Kung, K. Y. "A New Method of Correlation Studies of Pavement Deflection and Cracking." Proceedings, Second International Conference on the Structural Design of Asphalt Pavements, Ann Arbor, MI, 1967, pp. 1037-46.
24. Van Bramer, T. F. Performance of Two Rubber-Modified Asphalt-Concrete Overlays: A Three-Year Progress Report. Special Report 107, Engineering Research and Development Bureau, New York State Department of Transportation, December 1992.
25. Irwin, L. H. Instructional Guide for Back-Calculation and the Use of MODCOMP 3, Version 3.6 Report 92-5, Cornell Local Roads Program, Cornell University, July 1992.
26. Uzan, J., Michalek, C. H., Paredes, M. and Lytton, R. L. A Microcomputer Based Procedure for Backcalculating Layer Moduli from FWD Data. Research Report 113-1, Texas Transportation Institute, September 1988.
27. Anderson, M. "A Database Method for Backcalculation of Composite Pavement Layer Moduli." Special Technical Publication 1026, American Society for Testing and Materials, 1989, pp. 201-16.
28. Lytton, R. L., Germann, F. P., Chou, Y. J., and Stoffels, S. M. Determining Asphaltic Concrete Pavement Structural Properties by Nondestructive Testing. Report 327, National Cooperative Highway Research Program, Transportation Research Board, June 1990.
29. AASHTO Guide for Design of Pavement Structures: 1993. Washington: American Association of State Highway and Transportation Officials, 1993.

30. DARWin User's Guide: A Proprietary AASHTOWARE Computer Product. Savoy, IL: ERES Consultants, Inc., July 1991.
31. Stubstad, R. N., and Connor, B. "Use of Falling Weight Deflectometer to Predict Damage Potential on Alaskan Highways During Spring Thaw." Transportation Research Record 930, Transportation Research Board, 1983, pp. 46-51.